The Institute of Space and Astronautical Science
Report SP No. 16, March 2003

Comprehensive geochemical analyses of small amounts (< 100 mg) of extraterrestrial samples for the analytical competition related to the sample return mission MUSES-C

By

Eizo NAKAMURA*, Akio MAKISHIMA*, Takuya MORIGUTI*,
Katsura KOBAYASHI*, Chie SAKAGUCHI*, Tetsuya YOKOYAMA*,
Ryoji TANAKA*, Takeshi KURITANI*, and Hiroyuki TAKEI*

(1 February 2003)

Abstract: We have participated in the analytical competition related to the sample-return mission, MUSES-C of the ISAS, to be launched in May 2003 and returned in summer 2007. In this competition, we have determined major and trace element abundances and isotopes (as many as possible), both for two powdered samples provided by the ISAS and for chondrules separated from Allende meteorite as an additional demonstration of our high-spatial resolution analytical capabilities for fragment samples.

100 mg of each of the competition samples, 1C and 2C, were split into two fractions of approximately 30 and 70 mg for the determinations of elemental abundances and the isotope analyses, respectively. The bulk concentrations of 55 elements in each 30 mg sample were analyzed by quadruple-type ICP-MS and sector-type ICP-MS with analytical uncertainties better than 10% (1σ). B, Pb, Li, Rb, Sr, Sm and Nd were successively separated from the remaining 70 mg of each of the samples, using a novel integrated, multi-ion exchange column chemistry approach, and then the isotopes of these elements were successfully determined by TIMS with analytical errors similar to those for analyses of terrestrial samples. The Sr, Nd, Re and Os isotopic compositions were also analyzed using the remaining aliquots of the sample solutions for trace element analyses by ICP-MS. The results obtained in this study indicate that 1C and 2C samples are probably ordinary chondrite and the Allende meteorite, respectively. However, extreme W, Ta and Nb enrichments in the 1C were probably caused by contamination during sample preparation. Furthermore, both of the samples were extensively contaminated by B from the borosilicate glass container in which the samples were delivered.

Five chondrules were separated from Allende meteorite and then sliced into three pieces using a dicing saw. The center slices were used to petrographically determine the mineral phases, compositionally map these phases by SEM-EDX, and obtain quantitative major and trace element compositions (30 elements) by SEM-EDX and ion microprobe. The two outer slices, for which

* Corresponding author, Electoric mail: eizonak@misasa.okayama-u.ac.jp
The Pheasant Memorial Labratory for Geochemistry and Cosmochemistry, Institute for Study of the Earth's Interior, Okayama Universty at Misasa, Tottori 682-0193, JAPAN

sample masses were less than 1 mg, were chemically treated to obtain the bulk trace elements and isotope compositions of the chondrules. For the chondrule slices, 24 trace elements and Sr and Nd isotopic compositions were determined with extremely small analytical uncertainties by ICP-MS and TIMS (for Sr and Nd, respectively).

Based on our analytical experience, including this competition, we believe that all of the analyses we carried out could have been completed within 50 days if we could have concentrated on this project alone during that 50-day period. In this report, we describe the analytical techniques employed for the powdered samples and the chondrules, and we present all of the results obtained during the approximately 3-month period of the analytical competition.

1. INTRODUCTION

The only extraterrestrial body from which samples have been directly returned to the Earth is the Moon (i.e., other ones as meteorites). In order to investigate these precious lunar samples, mainly American scientists dramatically improved both analytical techniques and the overall performance of analytical facilities in the late 1960s to early 1970s. These advancements made precise geochemical, petrological and chronological studies possible, resulting in a drastic increase in our knowledge regarding the origin and evolution of the Moon. However, Japanese geochemists could not participate significantly in the study of these lunar samples during the early stages of the Apollo program, other than undertaking some petrological investigations, due to the relatively poor analytical techniques and facilities for trace element and isotope analyses on extremely small samples. Even in late 1980s, analytical capabilities in Japanese geochemistry and cosmochemistry laboratories were not at a satisfactorily international level even for trace element and isotope study of terrestrial samples.

In order to correct this gap in the analytical capabilities in geochemistry and cosmochemistry in Japan, we have developed a Comprehensive Analytical System for Terrestrial and Extraterrestrial Materials (CASTEM) in the Pheasant Memorial Laboratory (PML) at the Institute for Study of the Earth's Interior (ISEI), Okayama University at Misasa. CASTEM consists of a genuine all-fresh- and circulatory-type clean room system (overall size 350 m^2) and associated modern instrumentation including thermal ionization mass spectrometers (TIMS), inductively coupled plasma mass spectrometers (ICP-MS), SEM-EDX and XRF facilities, and ion microprobes. Details of CASTEM are provided on our homepage, http://pmlgw.misasa.okayama-u.ac.jp/. Our purpose in developing CASTEM has been to apply new and existing geochemical tracers in studies of terrestrial and extraterrestrial materials aimed at understanding the origin, evolution and dynamics of the Earth and the solar system. Our research involves the development of many new techniques for quantitative analyses of the abundance and isotopic compositions of ultra-trace elements, in many cases affording textural analysis at high spatial resolution. Such new data will provide indispensable information that will further our understanding of the origin and evolution of terrestrial bodies, such as the Earth, Moon, Mars, and asteroids. We believe that such an approach will be the guiding spirit of the analytical part of "Sample Return Projects from the Asteroids, Moon, and Mars" to be carried out by the Institute of Space and Astronautical Science (ISAS), the National Space Development Agency of Japan (NASDA), the National Aeronautics and Space Administration (NASA) and other agencies.

The CASTEM is now capable of analyzing about half of the elements in the periodic table by ICP-MS and TIMS. These analyses are performed with very high precision and with extremely low detection limits. Multi-isotope analyses by an array of TIMS (for as many as nine isotope systems), coupled with physical micro-sampling methods, and SIMS analyses for trace elements and isotopes, afford highly spatially resolved analyses important in modern geochem-

ical studies (see PML home page). Employing the CASTEM, we have been investigating many important geochemical and cosmochemical topics, including: mantle/crust recycling through subduction zones; mantle processes such as melt extraction, metasomatism and compositional layering; the evolution of mantle plumes and crustal materials; the evolution of meteorites; and determinations, based on high P-T experiments, of trace element partitioning between melt and solid and trace element diffusion in melts and solids. The most recent development of CASTEM involves extension of its analytical abilities for highly spatially resolved isotope analyses using a high-mass-resolution ion microprobe (Cameca ims-1270) installed in February, 2000.

In December 1999, the ISAS invited the community to participate in a competition to determine which laboratory will undertake the primary analysis of samples returned from an asteroid, by ISAS's MUSES-C mission in summer, 2007. This inspired us to apply our CASTEM to the asteroid samples, which could retain records of the materials in the earlier phase of the solar system, with less thermal alteration compared to the lunar samples because of the asteroid's size. We immediately decided to participate in the competition in order to demonstrate our analytical capabilities employing the CASTEM for extremely small amounts of samples. For this competition, we proposed to determine major and trace element abundances and as many isotopes as possible, for both powdered/bulk and fragment samples, and we requested 100 mg of each of the samples, the maximum weight allowed for the competition by ISAS.

1.1 Samples

Because the ISAS indicated the availability of materials for "destructive" or "non-destructive" analyses, we expected two different types of samples; a finely-ground homogeneous powder (for "destructive" analyses), and a rough powder containing small chunks of material (for "non-destructive" analyses), the latter of which is more likely to be obtained by the MUSES-C sampler based on the simulation experiments at ISAS. However, the two samples provided by ISAS (1C and 2C) were both powders, approximately 100 mg each with variable grain size smaller than 100 μm. These materials were contained in 0.3 mL vials made of borosilicate glass (Fig. 1), although we had proposed to perform B content and isotope analyses. The two samples, 1C and 2C, were gray and black in color, respectively, with the naked eye. Sample 1C contained fragments of crystals and composite-mineral grains such as chromian spinel ($\sim$20 μm), pyrrhotite ($\sim$20 μm), olivine associated with glass ($\sim$100 μm), and olivine + enstatite + glass + Fe-Ni metal ($\sim$50 μm). Sample 2C included fragments of chondrules (a few 10s to 150 μm) mainly consisting of olivine and diopside, and large olivine crystals up to 100 μm in diameter. We inspected several fragments separated from the samples employing our SEM-EDX system. However, we did not further investigate the fragments for their mineralogy, major element compositions, and trace element compositions using the ion microprobe, because it is difficult to obtain both bulk elemental and isotopic compositions, together with textural and mineral descriptions, for samples with grain sizes less than 150 μm. Instead, we worked on chondrules separated from the Allende meteorite as an additional demonstration of the capabilities we previously claimed in our proposal to ISAS.

A brief analytical flow chart for the powders and chondrules is provided in Fig. 2. The powdered samples were split into two fractions; approximately 30 mg for trace element analyses by ICP-MS and the rest ($\sim$70 mg) for Li, B, Sr, Nd and Pb isotope analyses by TIMS. Aliquots of the sample solutions used for trace element analyses by ICP-MS were used for the Sr, Nd and Os isotope analyses. Details of these analytical procedures are provided in the following sections. Allende chondrules, with grain size ranging from 1 to 2 mm in diameter, were sliced

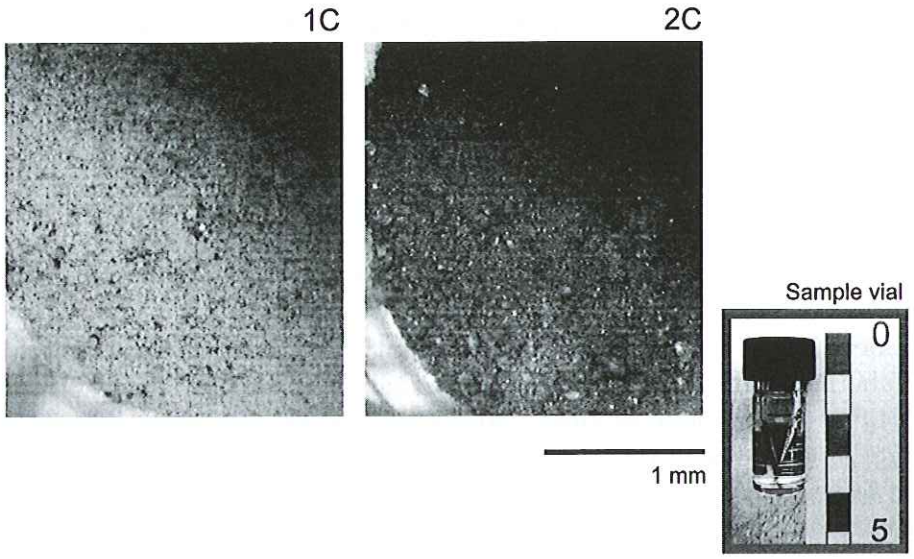

Fig. 1: Photographs of the competition samples, 1C and 2C, and the glass vial used to distribute the competition samples.

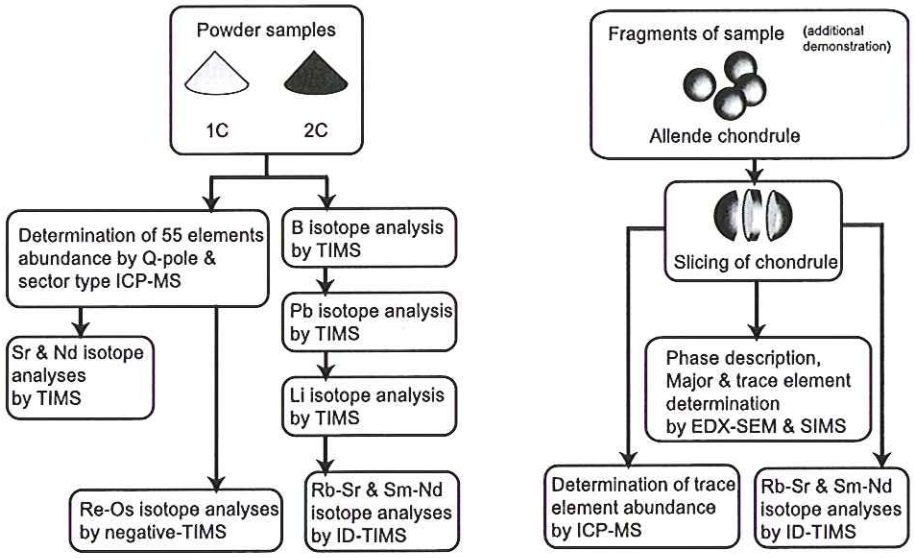

Fig. 2: Overview of the analytical sequence for the powder samples, 1C and 2C, and the Allende chondrules, analyzed as an additional demonstration.

into three pieces using a dicing saw. Then, the center portions were polished on glass slides for phase descriptions and major and trace element analyses by SEM-EDX and ion microprobe. The two outer portions were used for the bulk trace element analyses by ICP-MS, and for the Rb-Sr and Sm-Nd isotope analyses by TIMS. The analytical procedures for the chondrule analyses are also described in detail in the following sections.

2. GEOCHEMICAL ANALYSES FOR THE POWDERED SAMPLE (1C AND 2C)

2.1 Reagents and rock reference materials

Reagents

Water Three types of water, Milli-Q water, USQ water and 1D H_2O were used in this study. Milli-Q water was prepared by deionizing with a mixed-bed resin and filters (MILLIPORE). USQ water (*Ultra Super Milli-Q water*) was then purified by passing Milli-Q water through a Q-Pak cartridge equipped with 0.22 μm final filter (MILLIPORE). To further reduce the blank level in the water, especially for B, 1D H_2O was prepared as follows: 0.5 mL of B selective resin (Amberlite IR-743) and 2 g of mannitol (Merck) were added to 5 L of USQ, and stored three days with intermittent agitation. The supernatant was subsequently sub-boiled once by using a two-bottle Teflon still at a temperature of less than 80°C.

Hydrofluoric acid Analytical grade 46% HF (Wako), in which 1 g L^{-1} of mannitol was dissolved, was sub-boiled once using a two-bottle Teflon still. This was further sub-boiled in the two-bottle Teflon still, resulting in a 30M solution.

Hydrochloric acid EL grade (highly purified chemicals for the electronic industry) 36% HCl (Kanto Chemical) was diluted to 6M with Milli-Q water and sub-boiled once in a two-bottle Teflon still.

Hydrochloric acid for B isotope analysis For the B isotope analyses, HCl was prepared as follows: 35~37% HCl (B analysis grade; Wako) was diluted to 6M with water that was used for the preparation of 1D H_2O. This was sub-boiled once in a two-bottle Teflon still.

Cesium solution. Analytical grade Cs carbonate was dissolved in 0.1M HF to give a 9.25 $\times$ 10^{-3}M Cs solution. The solution was subsequently passed through 1 mL of AG 1X4 resin bed in F^- form to remove trace amounts of B.

Mannitol solution. Analytical grade mannitol powder was dissolved in 0.1M HF to obtain a 1% solution. This solution was passed through anion-exchange resin in the same way as employed for the cesium solution.

Phosphoric acid for B analysis 85% H_3PO_4 (Merck, Suprapur grade) was dissolved in 0.1M HF to obtain 3% H_3PO_4 solution. The solution was then passed through anion exchange resin in the same way as employed for the cesium solutions.

Nitric acid EL grade 69% HNO_3 (Kanto Chemical) was sub-boiled once in a two-bottle Teflon still, resulting in a 16M solution.

Hydrobromic acid. Analytical grade 47 $\sim$ 49% HBr (Kanto Chemical) was sub-boiled twice in a two-bottle Teflon still, resulting in a 8M solution.

Perchloric acid Highly purified 70% (7M) $HClO_4$ (TAMAPURE-AA-100) was used without further purification.

Aqueous ammonia Analytical grade aqueous ammonia (Kanto Chemical) was distilled in a two-bottle Teflon still at room temperature for ten days.

Pyridine Analytical grade pyridine (Merck) was sub-boiled once in a two-bottle Teflon still.

DCTA (1,2-cyclohexylenedinitrilotetraacetic acid monohydrate) Analytical grade DCTA (Merck) was used without further purification.

D.P.E (0.06M DCTA in 0.5M pyridine). DCTA was dissolved in distilled pyridine and diluted with Milli-Q, resulting in 0.06M DCTA in a 0.5M pyridine solution. The solution was passed twice through a cation resin bed column (Muromac AG 50WX12).

HIBA (α-hydroxyisobutyric acid) 208 g of analytical grade HIBA (Tokyo Kasei) was dissolved in 1L of 1D H_2O, and the solution was passed through 0.45 μm and 0.2 μm filters. The solution was subsequently purified by passing it once through cation exchange resin (Muromac AG 50WX12), resulting in a 2M solution. 2M HIBA was further diluted into appropriate concentrations (0.5M or 0.2M) by adding 1D H_2O and aqueous ammonia with adjusting pH to be approximately 5.

Ethanol Analytical grade 99.5% ethanol (Wako) was sub-boiled once using a two-bottle Teflon still at a temperature of less than 70°C.

Acetone Analytical grade 99.5% acetone (Wako) was sub-boiled once using a two-bottle Teflon still at a temperature of less than 60°C.

Rock reference materials

JB-2 In this study, we used a GSJ (Geological Survey of Japan) standard rock powder of JB-2 (tholeiitic basalt) as an elemental standard for ICP-MS analyses, and as a running standard for the TIMS analyses. JB-2 provided by GSJ was further pulverized, using an alumina ceramic swing mill, to minimize sample heterogeneity. Elemental concentrations for JB-2 were presented by Imai *et al.* (1995) for major elements, by Makishima & Nakamura (1997) for Rb, Sr, Y, Cs, Ba, REE, Pb, Th and U, by Makishima *et al.* (1997) for B, by Moriguti & Nakamura (1998) for Li, by Makishima *et al.* (1999) for Zr, Hf, Nb and Ta, by Makishima & Nakamura (1999) for Mo, Sb and W, and by Makishima &Nakamura (2000) for Ti. Isotopic compositions of JB-2 were presented by Koide & Nakamura (1990) for Pb, by Nakamura *et al.* (1992) for B, and by Moriguti & Nakamura (1998) for Li.

PML-Allende This sample, prepared at the PML, was used as another running standard for the TIMS analyses. Approximately 450g of an Allende meteorite block (a carbonaceous chondrite, CV3), donated by Mr. Sho Ito, was crushed into coarse chips with an iron hammer wrapped in plastic film. Fresh chips were carefully handpicked, and these chips were then further pulverized using a silicon nitride mortar and pestle.

Smithsonian-Allende In order to further assess our analytical performance in this study, we compared our analytical results with those for Smithsonian reference Allende powder (USNM3529, Split 1, Pos.23) determined in this laboratory by Makishima & Nakamura (1997) for Rb, Sr, Y, Cs, Ba, REE, Pb, Th and U, by Makishima *et al.* (1997) for B, by Makishima *et al.* (1999) for Zr, Hf, Nb and Ta, and by Makishima & Nakamura (1999) for Mo, Sb and W.

2.2 Comprehensive elemental analyses of the competition samples

Analytical strategy

For the comprehensive elemental analyses of the competition samples in this study, we classified 55 elements into three groups based on the chemical characteristics of the elements, and the analytical procedures employed for each group are indicated in Fig. 3. Group I included the alkali metals (Li, Na, K, Rb and Cs), alkaline earth elements (Mg, Ca, Sr and Ba), rare earths (Sc, Y, REE), transition metals (V, Mn, Fe, Co), Pb, Th and U. Most of these elements form insoluble fluorides during sample digestion with HF. Group II included B, Ti, Zr, Nb, Mo, Sn, Sb, Hf, Ta and W. In contrast with Group I, these elements form soluble oxo- or fluoro-complex anions in HF. Group III included siderophile and chalcophile elements such as S, Cr, Ni, Cu, Zn, Re and PGE (Ru, Pd, Os, Ir and Pt). In the following sections, we describe the details of the analytical procedures according to this grouping of elements (see Fig. 3).

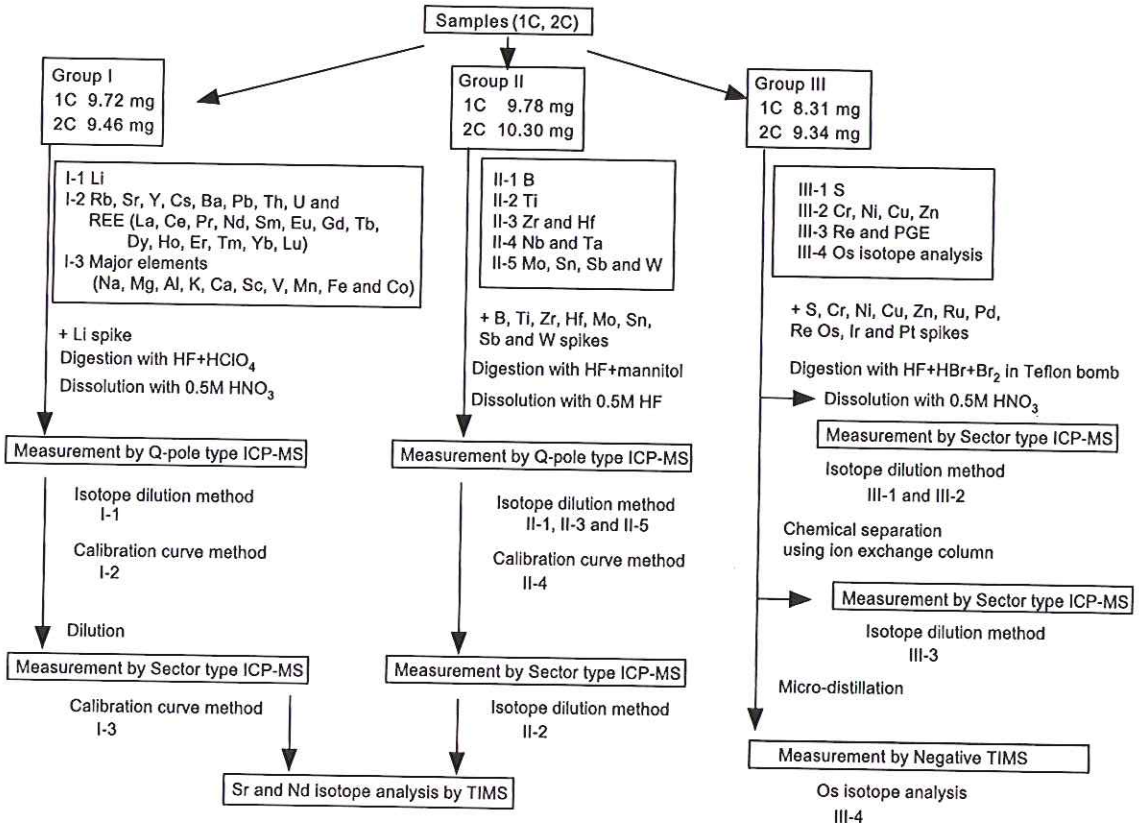

Fig. 3: Chemical procedure for comprehensive elemental analyses of the competition samples.

Analytical procedures

Group I (Li, Na, Mg, Al, K, Ca, Sc, V, Mn, Fe, Co, Rb, Sr, Y, Cs, Ba, REE, Pb, Th and U) We classified Group I elements into 3 sub-groups: I-1 (Li); I-2 (Rb, Sr, Y, Cs, Ba, REE, Pb, Th and U); and I-3 (Na, Mg, Al, K, Ca, Sc, V, Mn, Fe and Co). We used 9.72 mg and 9.46 mg of 1C and 2C, respectively, for the determinations of Group I elements.

Elements of Groups I-1 and I-2 were measured using an ICP mass spectrometer, the PMS 2000 (YOKOGAWA Analytical System, Japan) at PML, based on the methods of Moriguti *et al.* (in prep.) for Li, and Makishima & Nakamura (1997) for the other elements (with only slight modifications). The sample decomposition procedure was based on the method of Yokoyama *et al.* (1999).

In a clean room with a reduced static-electricity atmosphere, the two samples (1C and 2C) were weighed into clean 7 mL Teflon beakers followed by the addition of ^{6}Li-enriched spike (CMNM-IRM015; $^{7}Li/^{6}Li = 0.04545$; Li = 1.03 μg g^{-1}), resulting in $^{7}Li/^{6}Li$ ratio of ~0.5. Three beakers were separately prepared for the blank determinations, and these were treated the same as the beakers containing the samples. In the sample decompositions, 0.1 mL of 30M HF, 0.06 mL of 7M $HClO_4$ and 1 mL of USQ water were added to the beakers. After agitation of the beaker for 20 minutes in an ultrasonic bath, the capped beaker was heated at 100°C overnight on a hot plate in a draft chamber with extremely clean air(better than CLASS-100). The sample solution was then progressively evaporated at 120 °C for 6h and 150 °C for 6h. 0.06 mL of 7M $HClO_4$ and 0.06 mL of 16M HNO_3 were subsequently added to the beaker. The sample was again evaporated in a step-wise fashion at 120°C, 165°C and 195°C until dryness. 0.15 mL of 6M HCl were then added to the dried residue and it was evaporated at 120°C. Finally, the sample was dissolved into 2.5 mL of 0.5M HNO_3 and used for ICP-MS analyses (analytical method described below).

In the ICP-MS analyses, ICP operation at high power (1.7 kW) and a flow injection sample introduction system were employed for the suppression of matrix effects (Makishima & Nakamura, 1997). A micro-concentric nebulizer, MCN-100 (CETAC Technologies Inc., Nebraska, USA), was used in order to minimize sample usage. Li determination was carried out in triplicate for each sample using an isotope dilution technique (Moriguti *et al.*, in prep.). The other elements were also analyzed in triplicate with a calibration curve method by using 20 mg of JB-2 decomposed as described above for the standard material (Makishima & Nakamura, 1997). In both cases, approximately 0.15 mL of the sample solution was required for each analysis. Therefore, ~0.9 mL of the solution was consumed in these analyses for each sample, and the remaining solution (~1.6 mL) was used for the analyses of major element concentrations and the isotope measurements of Sr and Nd.

0.2 mL of the sample and JB-2 solutions were further diluted to 2 mL with 0.5M HNO_3. Using a sector-type ICP mass spectrometer, ELEMENT (Finnigan MAT GmbH, Germany) at mass resolution of 7500, the Group I-3 elements (Na, Mg, Al, K, Ca, Sc, V, Mn, Fe and Co) were measured by a calibration curve method (Kobayashi *et al.*, in prep.), using the diluted JB-2 solution as a standard solution.

Group II (B, Ti, Zr, Nb, Mo, Sn, Sb, Hf, Ta and W) We classified Group-II elements into 5 sub-groups: II-1 (B); II-2 (Ti); II-3 (Zr and Hf); II-4 (Nb and Ta); and II-5 (Mo, Sn, Sb and W). We used 9.78 mg and 10.30 mg of 1C and 2C, respectively, for the determinations of the Group II elements.

Samples with B-Ti-Zr-Sn-Sb-Hf-W spikes were decomposed in HF and mannitol in an ultra-

sonic bath, evaporated and re-dissolved by 0.5M HF leaving Mg and Al fluorides residues. This HF solution was directly nebulized into an ICP-MS, PMS-2000 (Yokogawa Analytical Systems, Japan) for the determinations of B, Zr-Nb-Hf-Ta, Mo-Sb-W and Sn. Details of the analytical procedures for B, Zr-Nb-Hf-Ta, Mo-Sb-W and Sn are, or will be, described in Makishima *et al.* (1997), Makishima *et al.* (1999), Makishima & Nakamura (1999) and Makishima & Nakamura (in prep.). The HF sample solution was also directly nebulized into the sector type ICP-MS, ELEMENT for the determination of Ti at mass resolution of 3000. Details of the analytical methods for Ti analyses are described in Makishima & Nakamura (2000).

External calibration curve methods were applied to the Group II-4 elements, and isotope dilution methods (ID) were applied in the determinations of Group II-1, II-2, II-3 and II-5 elements.

Group III (S, Cr, Ni, Cu, Zn, Ru, Pd, Re, Os, Ir and Pt) We classified Group III elements into 4 sub-groups: III-1 (S); III-2 (Cr, Ni, Cu and Zn); III-3 (Re, Ru, Pd, Ir and Pt); and III-4 (Os). We used 8.31 mg and 9.34 mg of 1C and 2C, respectively, for the determinations of the Group III elements.

The competition samples with S-Cr-Ni-Cu-Zn-Ru-Pd-Re-Os-Ir-Pt spikes were digested by a mixed acid solution of HF and HBr, and subsequently decomposed at 245°C in a Teflon bomb. In this procedure, all sulfides and spinel, which are major hosts of these elements, are completely decomposed while achieving isotope equilibria between the sample and spike. After drying, parts of the sample solution were dissolved with 0.5M HNO_3 and centrifuged. The supernatant was directly aspirated into the sector-type ICP-MS, ELEMENT, to determine Group III-2 elements by isotope dilution methods at a mass resolution of 7500. The solution was further diluted, and S was determined by ELEMENT at a mass resolution of 3000. Details of the analytical procedures will be described in Makishima & Nakamura (2001) and Makishima *et al.* (2002).

Group III-3 and III-4 elements in the remaining aliquots of the HNO_3 solutions were separated and purified by ion exchange chemistry into III-3 and III-4 fractions (Makishima *et al.*, 2001). Group III-3 and III-4 elements were determined by ELEMENT at a mass resolution of about 500 using isotope dilution techniques.

The III-4 fractions were further treated and $^{187}Os/^{188}Os$ ratios were determined as described in section 2.4 (Makishima & Nakamura, in prep.).

Results and discussion

Results of the comprehensive elemental analyses, together with those of the Smithsonian-Allende powder obtained in our lab and by Jarosewich *et al.* (1987), are shown in Table 1. All of the analytical results obtained by calibration curve methods are based on the concentration of the elements in JB-2, which are determined independently by ourselves and also recommended by Imai *et al.* (1995). These values are provided in Table 1.

Maximum blank corrections (%) and uncertainties (1σ%) estimated by numerous analyses of standard and natural rock samples in our laboratory are also shown in Table 1, as are the CI chondrite values of Anders & Grevesse (1989).

Element abundances for the competition samples are normalized to CI chondrite (Anders & Grevesse, 1989) and shown in Fig. 4. The 1C sample shows Cs and Pb depletion and strong Nb, Ta and W enrichment relative to CI. Siderophile and chalcophile elements such as S, Co, Ni, Cu, Mo, Sb, PGE are also depleted in the 1C sample. In contrast, refractory lithophile

elements such as Al, Ca, Sc, Ti, Zr, REE, Hf, Ta, Th and U show smooth patterns within a factor of 1-2 of CI concentrations. Based on these observations, we conclude that (1) the 1C sample is probably an ordinary chondrite because it has smooth refractory element patterns, including for REE, with abundances similar to CI, and depletion of volatile Cs and Pb relative to CI; (2) there is a possibility of contamination during the powder preparation resulting in enrichment of W, Ta and Nb. If the source material of the 1C sample was an ordinary chondrite, W, Ta and Nb enrichments were probably caused by contamination, because (i) selective enrichment of these elements is difficult to achieve as a result of natural processes, and (ii) the Nb/Ta ratio of the 1C sample is 1.7, which is far lower than that in natural samples (usually 10–20, even in meteorites). We consider it likely that the 1C sample was prepared by crushing an ordinary chondrite using a tungsten-carbide mortar and pestle, resulting in the W, Ta and Nb enrichments. If such a sample-grinding method is applied, care should be taken in instrumental neutron activation analyses (INAA), one of the most popular methods for elemental analyses. For INAA, W and Ta contamination produces higher backgrounds and severe photopeak interferences to not only W and Ta, but also REE and especially Eu Tm, and Lu (see Potts, 1987).

In contrast with the 1C sample, the 2C sample shows a relatively smooth chondrite-normalized pattern, and its REE abundances are twice as high as those of CI. These characteristics are typical for the Allende meteorite. The slight depletion of volatile Cs and Pb also fits this hypothesis. The element abundances of the Smithsonian-Allende powder vs. those for the 1C and 2C samples, most of which were determined by our laboratory, are shown in Fig. 5. There is a good correlation between the 2C sample and Smithsonian-Allende over a wide compositional range of 0.02 to 300000 μg g^{-1}. This plot clearly shows that the 2C sample has the element abundances of Allende.

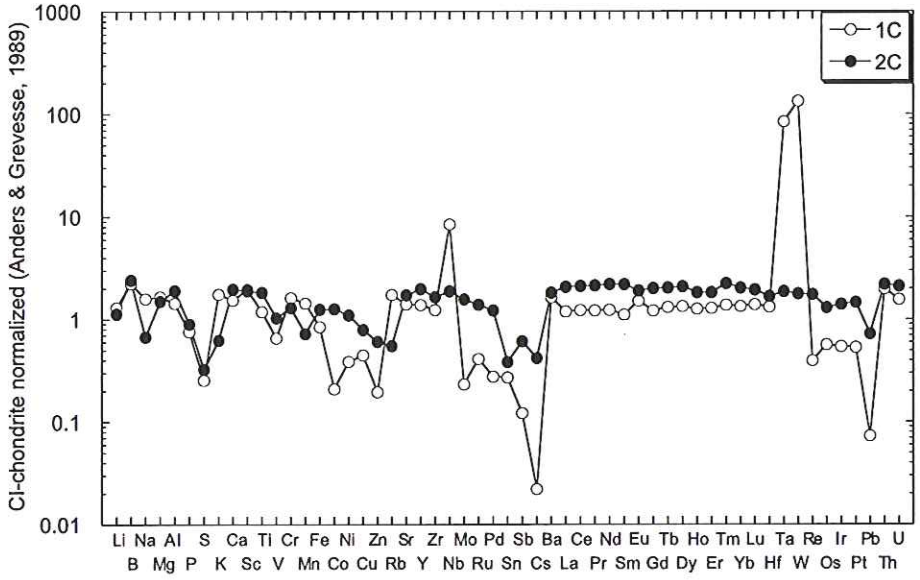

Fig. 4: CI-chondrite normalized element abundances of the competition samples.

Table 1: Element abundances (μg g^{-1}) of competition samples, CI chondrite, JB-2 and Smithsonian Allende.

Element	Group	1C	2C	Blank correction(%)	Uncertainty (1σ)%	CI chondrite (Anders & Grevesse, 1989)	JB-2	ref.	Smithsonian Allende	ref.
Li	I-1	1.96	1.70	<2.5	<3	1.50	7.75	6	1.63	6
B	II-1	1.95	2.11	<3	<3	0.870	31.3	1	1.07	1
Na	I-3	7980	3370	<1	<10	5000	15100	10	3410	10
Mg	I-3	165000	149000	<1	<10	98900	27900	11	148000	10
Al	I-3	12500	16600	<1	<10	8680	77400	11	17400	10
P	I-3	928	1100	<1	<10	1220	440	11	1050	10
S	III-1	16000	20400	<1	<10	62500	18.9	12	20400	12
K	I-3	984	348	<1	<10	558	3490	11	332	10
Ca	I-3	14300	18300	<1	<10	9280	70200	11	18447	10
Sc	I-3	11.4	11.1	<1	<10	5.82	53.5	11	11	10
Ti	II-2	519	799	<1	<5	436	6830	5	899	5
V	I-3	37.0	58.4	<1	<10	56.5	575	11	92	10
Cr	III-2	4330	3450	<1	<10	2660	25	8	3704	8
Mn	I-3	2870	1440	<1	<10	1990	1690	11	1471	10
Fe	I-3	161000	238000	<1	<10	190400	99600	11	235700	10
Co	I-3	106	637	<1	<10	502	38.0	11	600	10
Ni	III-2	4270	12100	<1	<10	11000	14.2	8	14200	8
Cu	III-2	56.6	99.4	<1	<10	126	230	8	112	8
Zn	III-2	61.0	189	<1	<10	312	113	8	115	8
Rb	I-2	3.50	1.11	<2.5	<4	2.30	6.22	7	1.34	2
Sr	I-2	11.0	13.4	<2.5	<4	7.80	177	2	14.2	2
Y	I-2	2.16	3.10	<2.5	<4	1.56	25.9	2	3.14	2
Zr	II-3	4.87	6.50	<1	<5	3.94	46.0	3	6.24	3
Nb	II-4	2.09	0.465	<1	<5	0.246	0.430	3	0.375	3
Mo	II-5	0.217	1.46	<1	<5	0.928	0.895	4	1.42	4
Ru	III-3	0.293	0.990	<1	<10	0.712			1.04	9
Pd	III-3	0.155	0.685	<3	<10	0.560			0.716	9
Sn	II-5	0.467	0.659	<8	<8	1.72	0.719	8	0.3	10
Sb	II-5	0.0174	0.0866	<1	<5	0.142	0.214	4	0.0743	4
Cs	I-2	0.00415	0.0789	<2.5	<4	0.187	0.794	2	0.0847	2
Ba	I-2	3.83	4.27	<2.5	<4	2.34	229	2	4.95	2
La	I-2	0.281	0.487	<2.5	<4	0.235	2.19	2	0.465	2
Ce	I-2	0.744	1.28	<2.5	<4	0.603	6.43	2	1.15	2
Pr	I-2	0.109	0.191	<2.5	<4	0.0891	1.13	2	0.179	2
Nd	I-2	0.560	1.000	<2.5	<4	0.452	6.39	2	0.940	2
Sm	I-2	0.164	0.323	<2.5	<4	0.147	2.27	2	0.310	2
Eu	I-2	0.0850	0.107	<2.5	<4	0.0560	0.855	2	0.104	2
Gd	I-2	0.240	0.397	<2.5	<4	0.197	3.12	2	0.459	2
Tb	I-2	0.0477	0.0740	<2.5	<4	0.036	0.592	2	0.0713	2
Dy	I-2	0.325	0.508	<2.5	<4	0.243	4.13	2	0.497	2
Ho	I-2	0.0705	0.102	<2.5	<4	0.0556	0.898	2	0.106	2
Er	I-2	0.204	0.291	<2.5	<4	0.159	2.47	2	0.286	2
Tm	I-2	0.0334	0.0542	<2.5	<4	0.0242	0.392	2	0.0558	2
Yb	I-2	0.218	0.330	<2.5	<4	0.163	2.60	2	0.328	2
Lu	I-2	0.0340	0.0474	<2.5	<4	0.0243	0.397	2	0.0484	2
Hf	II-3	0.138	0.174	<1	<5	0.104	1.45	3	0.188	3
Ta	II-4	1.20	0.0266	<13	<13	0.0142	0.0327	3	0.0203	3
W	II-3	12.4	0.165	<2	<5	0.0926	0.299	4	0.159	4
Re	III-3	0.0144	0.0640	<4	<10	0.0365			0.0733	9
Os	III-4	0.275	0.631	<1	<10	0.486			0.796	9
Ir	III-3	0.261	0.674	<1	<10	0.481			0.750	9
Pt	III-3	0.528	1.45	<1	<10	0.990			1.59	9
Pb	I-2	0.181	1.78	<2.5	<4	2.47	5.28	2	1.69	2
Th	I-2	0.0587	0.0646	<2.5	<4	0.0294	0.277	2	0.0646	2
U	I-2	0.0127	0.0171	<2.5	<4	0.00810	0.166	2	0.0169	2

References: 1. Makishima *et al.* (1997); 2. Makishima &. Nakamura (1997); 3. Makishima *et al.* (1999); 4. Makishima & Nakamura (1999); 5. Makishima & Nakamura (2000); 6. Moriguti *et al.* (in prep.); 7. Sakaguchi (unpublished data); 8. Makishima *et al.* (2002); 9. Makishima & Nakamura (in prep.); 10. Jarosewich *et al.* (1987); 11. Imai *et al.* (1995); 12. Makishima & Nakamura (2001)

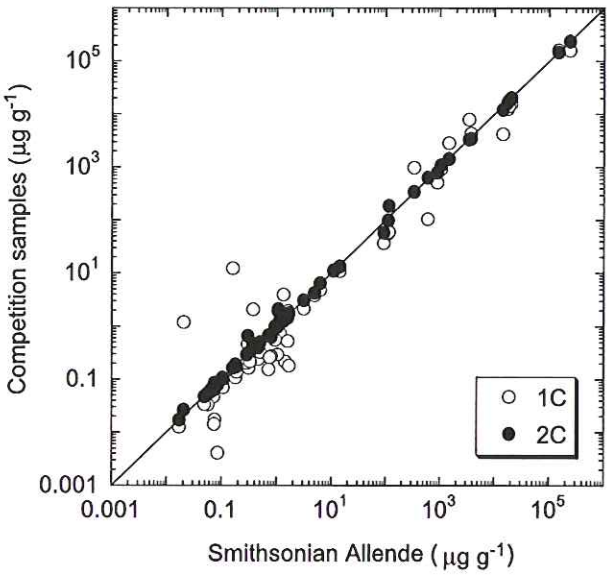

Fig. 5: Composition of elemental abundances between Smithsonian-Allende and the competition samples.

2.3 B, Pb, Li, Sr and Nd isotope analyses

Chemical separation

Dissolution of powdered sample The competition samples (1C and 2C), together with standard rock sample JB-2 (supplied by the GSJ) and two samples of PML-Allende powder, were simultaneously processed in the series of isotope analyses of B, Pb, Li, Sr, Nd, Rb and Sm separated from the ~70 mg samples (Fig. 6) The chemical separation procedures independently developed for the various isotope systems in our laboratory (Nakamura *et al.*, 1992; Kuritani & Nakamura, 2002; Moriguti & Nakamura, 1998; Yoshikawa & Nakamura, 1993; Makishima *et al.*, 1991) were fully integrated, and the order of chemical separation using ionic exchange chromatography was arranged to minimize the loss of recovery yields of each element during the overall procedure. The sequence of chemical separations of these elements is presented in Fig. 6 as a flow chart.

For simultaneous determination of Sr and Nd isotopic compositions and Rb, Sr, Nd and Sm concentrations, we prepared a mixed spike solution enriched in ^{87}Rb, ^{150}Nd and ^{149}Sm, provided by Oak Ridge National Laboratory, and ^{84}Sr (NIST SRM 988) in 1.0M HCl. Three types of mixed spike solutions (M1, M2 and M3) were prepared to be adapted to various concentrations of these four elements in natural samples. The concentrations and isotopic ratios of the four elements in these mixed spikes are shown in Table 2. Mixed spike M1 was used for isotopes and quantitative analyses of powdered 1C, 2C, PML Allende and JB-2. Mixed spikes M2 and M3 were used for the analyses of chondrules described in Section 3. The concentrations of the elements in the mixed spike solutions were defined to minimize the error magnification factor for the analyses of samples compositions similar to chondritic values in the isotope dilution mass spectrometry.

In order to reduce the B blank in the mixed spike solution by the emission of BF_3 gas, 0.06 mL of 30M HF was added to the precisely weighed spike solution in a Teflonbeaker without

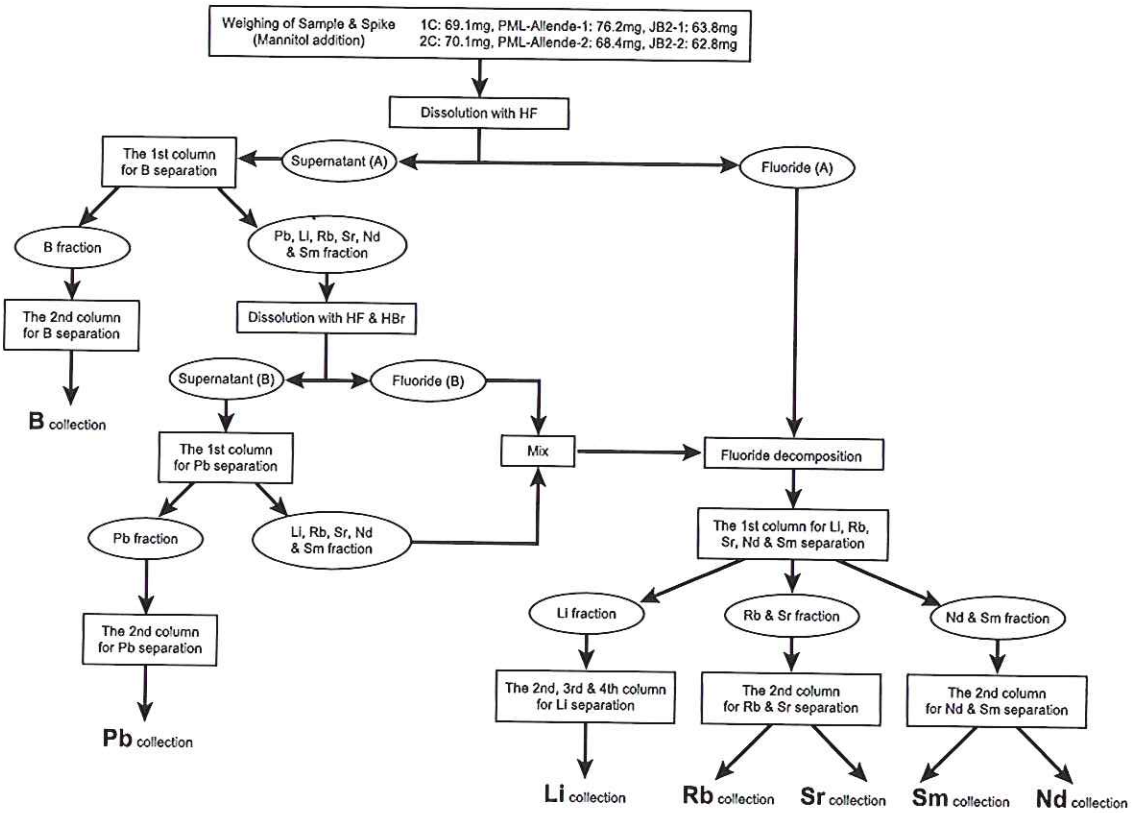

Fig. 6: Flow chart of chemical separations of B, Pb, Li, Rb, Sr, Sm and Nd from the samples.

Table 2: Concentrations and isotope ratios of mixed spike solutions.

	concentration (μg g^{-1})			
type	Sr	Rb	Nd*	Sm*
M1	0.0604	0.966	0.00142	0.00370
M2	0.0943	0.147	0.000214	0.000504
M3	0.0152	0.0233	0.0000339	0.0000840

	Isotope ratio			
	^{84}Sr/ ^{86}Sr	^{87}Rb/^{85}Rb	^{150}Nd/^{144}Nd	^{149}Sm/^{147}Sm
	1713.635	48.43	195.262	74.75

*) These values represent "pseudo" concentrations (P) defined as follows:
$P = C \times (D_{spike} / D_{sample}) \times (M_{sample} / M_{spike})$
where C, D_{spike}, D_{sample}, M_{sample} and M_{spike} are the concentration of spike, atomic abundances of spike and sample, and atomic masses of sample and spike, respectively.

addition of mannitol solution, then dried at 80°C prior to the sample weighing. B has a strong affinity with fluorine, and forms highly volatile BF_3 gas (Ishikawa & Nakamura, 1990). The sample was then precisely weighed, and 0.2 mL of mannitol solution was added to the sample to further reduce the B content of the sample (Ishikawa & Nakamura, 1990; Nakamura *et al.*, 1992). The sample was then dissolved with 2 mL of 30M HF. The tightly sealed Teflon beaker containing the sample was agitated using an ultrasonic bath until the rock powder nearly disappeared. The final dissolution was then accomplished by heating overnight at 70°C.

After complete dissolution, as determined by visual inspection, the beaker was centrifuged. The supernatant was transferred into a clean Teflonbeaker. After that, the residual fluorides were rinsed twice with 2 mL of 30M HF and the supernatant HF solutions were added to the previously collected supernatant (Supernatant (A) in Fig. 6). The Supernatant (A) was evaporated to dryness at 70°C. The dried sample was then dissolved with 0.5 mL of 6M HCl and subsequently evaporated to dryness at 70°C in order to convert the sample to chloride for the first-column stage of the B separation process (Nakamura *et al*, 1992). Insoluble fluorides (Fluoride (A) in Fig. 6) obtained after the centrifugation contain large portions of the Li, Rb, Sr, Nd and Sm in the sample (Moriguti & Nakamura, 1998; Yokoyama *et al.*, 1999). Moreover, the precipitation of the fluorides may cause a large isotopic fractionation of Li between the fluorides and the solution. In order to achieve complete recovery yields of these elements, the fluorides were recovered and decomposed as described in the following section.

Separation of boron The analytical procedures for B purification are the same as those described in Nakamura *et al.* (1992). 1 mL of 0.1M HCl was added to the dried supernatant (A) (Fig. 6). The solution was agitated using an ultrasonic bath and then centrifuged. B in the chloride-form supernatant was chemically isolated from the sample in two stages; (1) removal of other elements using cation exchange resin in the H^+ form, and (2) purification of B using anion exchange resin in the F^- form. The residue containing insoluble fluoride was transferred to the beaker containig Fluoride (A) with 1.5 mL of 6M HCl.

3.0 mL of cation exchange resin (AG 50WX12, 200-400 mesh) were loaded onto a polypropylene column (4.2 mm in diameter × 55 mm in length). The resin bed was cleaned with 6M HCl and 1D H_2O. The sample solution was loaded onto the cation-exchange column. The B fraction was subsequently collected using 5.5 mL of 1D H_2O. Afterwards, other elements, including Pb, Li, Rb, Sr, Sm and Nd, were collected as a fraction using 25 mL of 6M HCl. 0.2 mL of 3% phosphoric acid (prepared for B work; see Section 2.2) were added to the B fraction and the solution was evaporated at 70°C.

0.3 mL of anion-exchange resin (AG 1X4, 200-400 mesh) was loaded onto a polypropylene column (3.0 mm in diameter × 40 mm in length) and cleaned with 6M HCl and H_2O. 0.6 mL of 3M HF was added to the evaporated sample, and the solution was loaded onto the anion-exchange column. Subsequently, 1.5mL of mixed acid composed of 2M HCl and 0.5M HF was added to the column. The B fraction was then collected using 1.7 mL of 6M HCl. The B was collected in a Teflon beaker containing 200 μg of mannitol, obtained from 1% mannitol solution and 0.2 mL of 3% phosphoric acid, and this solution was then evaporated at 70°C. Although major elements and most of the trace elements are separated from B in the anion exchange chromatography, trace amounts of Nb, Mo, and W still remained in the B fraction. Therefore, the B was repeatedly purified using the same anion-exchange column. Finally, the B was collected in a concave-bottom Teflon beaker containing Cs solution and mannitol solution to give the B/Cs mole ratio of 2 and 40-50 μg of mannitol/1μg of B. The total recovery yield was determined to be >99% (Nakamura *et al.*, 1992).

Separation of lead The sample solution containing the Pb, Li, Rb, Sr, Nd and Sm from the first column chemistry of the B separation, was dried completely in a closed evaporation system (see our homepage). The dried sample was dissolved in 0.5 mL of HF and 0.5 mL of HBr in a 7 mL PFA Teflon beaker. To promote the reactions, the samples mixed with acids were decomposed using an ultrasonic bath (for about 8 hours). The resulting solutions were then heated for several hours at 110°C on a hot plate in a clean evaporator equipped with a cleaned air flow system. The completely decomposed samples were then evaporated to dryness at 110°C. The dried samples were dissolved in 1 mL of 0.5M HBr and the solutions were subsequently centrifuged to remove fluoride deposits (Fluoride (B) in Fig. 6) precipitated during the decomposition.

0.1 mL of anion exchange resin, Bio-Rad AG 1X8, was charged into a polyethylene column (3.8 mm in diameter × 8.8 mm in length.). The resin bed was cleaned by flushing the column with 1.5 mL of 0.5M HNO_3 followed by 1.5 mL of USQ water. The column was then conditioned with 0.3 mL of 0.5M HBr. The Supernatant (B) (Fig. 6) of the dissolved sample was loaded onto the column, with care taken not to introduce the fluoride deposits. Then 2.5 mL of 0.25M HBr – 0.5M HNO_3 mixed acid was introduced for removal of elements other than Pb. The solution that flowed out from the columns was collected and used for separations of Li, Rb, Sr, Nd and Sm. This solution was mixed with the Fluoride (B). The solution plus Fluoride (B) was decomposed as described in the following section. The Pb was eluted by 1.0 mL of USQ water. To avoid complete dryness, 0.03 mL of 0.05M H_3PO_4 was added to the elute prior to evaporation.

For sample 1C, in which the Pb content is as low as 12 ng Pb, a second column chemistry was carried out to reduce the amount of impurities relative to that of the sample Pb. A 10 μL-column (1.5 mm in diameter × 5.7 mm in length) was used in this column chemistry. The anion-exchange resin was charged into the column, and the resin bed was cleaned by flushing the column with 0.3 mL of 0.5M HNO_3 and 0.3 mL of USQ water. The column was then conditioned with 0.1 mL of 0.5M HBr. The dried sample collected from the first column was dissolved in 0.3 mL of 0.5M HBr, and was loaded onto the column. For washing of organic materials, 0.3 mL of 0.5M HBr was introduced. Subsequently, 0.3 mL of USQ water was added to the column as a Pb elution. The collected Pb fraction was evaporated in a closed system at 80°C for several hours, after addition of one drop of 0.05M H_3PO_4 in order to avoid complete dryness.

Preparation for separation of lithium, rubidium, strontium, samarium, and neodymium A combination of perchloric acid addition and drying by step-wise heating is effective in completely decomposing insoluble fluorides (Yokoyama *et al.*, 1999), and this method was adopted in this study. 0.5 mL of $HClO_4$, 0.45 mL of HF and 0.3 mL of HNO_3 were added to the residue including the Fluoride (A). The tightly capped beaker was heated at 100°C for 12 hours. The resulting solution was evaporated at 120°C for 12 hours, 165°C for 12 hours and 195°C until dryness in a closed system. The sample was then dissolved using 0.45 mL of $HClO_4$ and was dried in the same step-wise fashion in a clean evaporator equipped with a cleaned air flow system.

The collected fraction containing Li, Rb, Sr, Nd and Sm from the first column of the Pb separation process was transferred to the beaker containing the Fluoride (B) and was evaporated to dryness at 120°C. 0.15 mL of 7M $HClO_4$ was added to the dried sample and evaporated to dryness by the step-wise heating method. The resulting dried sample was dissolved with 0.35 mL of 6M HCl and then transferred to the beaker containing decomposed Fluoride (A).

The resulting solution containing all fractions of Li, Rb, Sr, Nd and Sm resulting from this comprehensive chemical separation process was evaporated to dryness at 120°C. Subsequently, the dried sample was dissolved in 1 mL of 4M HCl for the cation-exchange chemistry for rough separation of these five elements.

Separation of lithium The Li separation procedure consisted of four steps (Moriguti & Nakamura, 1998). In the first, second and third column stages, a polypropylene 1 mL volume size (5.0 mm in diameter × 50 mm in length) column was used and in the fourth column stage, polyethylene 0.1 mL volume size (3.8 mm in diameter × 8.8 mm in length.) column was used. A sulfonated polystyrene cation-exchanger, Muromac AG 50WX12 (200-400 mesh), was used in all stages.

In the first column stage, major elements were roughly removed. The column was conditioned with 1mL of 4M HCl after resin washing with 20 mL of 6M EL HCl, 10 mL of Milli-Q water, 10 mL of 0.15M HF, 20 mL of 6M HCl and 10 mL of 1D-H_2O. The 1 mL of 4 M HCl loading solution obtained as described in the previous section (2.3) was loaded onto the column. 2.5 mL of 2.8M HCl was then introduced into the column. The entire 3.5 mL of effluent was collected as a Li fraction. This Li sample solution was then evaporated to dryness at 120°C.

In the second column stage, Li and Na was separated from the other major elements. The column was conditioned with 1 mL of 1D H_2O after resin washing by the same procedure as that used in the first column stage. The dried sample obtained from the first column stage was dissolved with 2 mL of 0.15M HCl, and the resulting solution was loaded onto the column. 17.5 mL of 0.15M HCl was then introduced into the column, and the entire 19.5 mL of effluent was collected. This Li fraction was then dried at 120°C. The dried volumes of the Li fractions of 1C, 2C and PML-Allende were significantly larger than those of common terrestrial samples. In order to prevent a matrix effect in the third column chemistry, the second column stage was repeated for these samples.

In the third column stage, Na was removed. The column was conditioned with 1 mL of water after resin washing by the same procedure as that used in the first column stage. The dried sample was dissolved in 1 mL of 0.15M HCl and loaded onto the column. 9 mL of 30 vol.% ethanol in 0.5M HCl was added to the column. The entire 10 mL of effluent was then collected and evaporated to dryness.

In the fourth column stage, organic materials (derived mainly from the resin) and V are removed. The column was conditioned with 1 mL of 1D H_2O after resin washing by 1 mL of 0.15M HF, 2 mL of 6M HCl and 1 mL of 1D H_2O. The dried sample was dissolved in 0.1 mL of 0.06M HCl and loaded onto the column. Then 0.5 mL of water was loaded and then 0.4 mL of 0.15M HCl was added to the ion exchange resin bed to remove organic materials and V. The 1.8 mL of 0.15M HCl effluent was recovered as a final Li fraction.

In order to produce Li phosphate (Li_3PO_4) as an ion source material for the mass spectrometry, 12 μL of 0.017M phosphoric acid (H_3PO_4) was added to the final sample solution. Then the solution was evaporated on a hot plate at 90°C for a few hours.

Separation of rubidium, strontium, neodymium and samarium Methods for the chemical separation of Rb and Sr, and of Sm and Nd are essentially the same as those employed in Yoshikawa & Nakamura (1993) and Makishima & Nakamura (1991b), respectively. After Li collection, and in the first column stage, a fraction of Rb and Sr was collected with 5.5 mL of 2.8M HCl and subsequently a fraction of Sm and Nd was collected with 5.5 mL of 6M HCl. These fractions were dried at 110°C in the closed-system evaporator.

In the second column stage of the Rb and Sr separation process, Rb and Sr are purified in pyridinium form. 0.5 mL of resin was removed from the 1 mL column used at the first column stage after collection of the Nd and Sm fraction. The resin bed was then successively cleaned with 20 mL of 6M EL HCl, 10 mL of 1.5M HF, 10 mL of Milli-Q water, 20 mL of 6M 1D HCl and 10 mL of 1D H_2O. The resin was then conditioned with 0.5 mL of 25% pyridine. The dried fraction of Sr and Rb from the first column stage was converted to pyridinium chloride by adding 0.1 mL of 25% pyridine addition and dried at 60°C, and then dissolved in 3 mL of D.P.E.. This solution was loaded onto the column. 3 mL of D.P.E., 4 mL of 1D H_2O and 0.5 mL of 1.5M HCl were then successively added to the column to remove Mg, Ca and pyridine. Subsequently the Rb fraction was collected with 1mL of 2.8M HCl. 1 mL of 2.8M HCl was then added to the column in order to elute out the minor mix fraction of Rb and Sr. Sr was finally eluted by 2 mL of 6M HCl. These Rb and Sr fractions were evaporated to dryness at 110°C in the closed-system evaporator. 0.03 mL of 30M HF and 0.03 mL of 16M HNO_3 were added to each dried sample in order to break down organic materials mainly from D.P.E. and then these solutions were again dried at 110°C in the closed-system evaporator.

In the second column stage of the Nd and Sm separation process, Nd and Sm was purified with HIBA. 0.3 mL of Teflon column (3 mm in diameter × 40 mm in length) charged with 0.3 mL of cation-exchange resin, Muromac AG 50WX8, was used. The resin was washed with 1.5 mL of 0.5M HIBA and 1 mL of 1D H_2O, and then conditioned with 0.8 mL of 0.2M HIBA prior to sample loading. The dried sample including Nd and Sm from the first column stage was dissolved with 0.06 mL of 0.06M HCl. This solution was loaded onto the resin bed and 0.6 mL of 0.2M HIBA was added. The Sm fraction was then collected with 1.2 mL of 0.2M HIBA. Then 0.7 mL of 0.2M HIBA was added to the column in order to elute out the minor mix fraction of Sm and Nd. The Nd fraction was then collected with 2.5 mL 0.2M HIBA. These fractions of Sm and Nd were dried at 110°C in the closed-system evaporator. 0.03 mL of 30M HF and 0.03 mL of 16M HNO_3 were added to each dried sample in order to break down organic materials mainly from HIBA and then these solutions were dried at 110°C in the closed-system evaporator.

Mass spectrometry

Isotopic measurements were made using solid-source thermal ionization mass spectrometers, the modified Finnigan MAT 261 equipped with nine Faraday cup collectors, "KIJI", (Nakano & Nakamura, 1998) for B and Li, and the Finnigan MAT 262 equipped with five Faraday cup collectors, "TARO", for Pb, Sr, Nd, Rb and Sm. In both mass spectrometers, a Faraday cup collector was used with a $10^{11}\Omega$ resistor which is capable of detecting ion currents from 10^{-14} to 10^{-10} A for isotopic determinations. The accelerating voltage was adjusted to 8 kV for the B isotope analysis and 10 kV for the other isotopes analyses.

Boron The $Cs_2BO_2^+$-graphite method was used in our measurements (Nakamura *et al.*, 1992; Nakano & Nakamura, 1998). Prior to sample loading, trapezoid-shaped Ta filaments (2 mm top × 0.025 mm thickness × 0.75 mm width) were degassed for 30 minutes with a filament current of 3.0 A at 10^{-6} Torr in a degassing unit. The top of the filament was coated with approximately 40 μg of graphite, and then the B sample dissolved in 1 μL of 1D H_2O was loaded on the graphite layer to make a sample-graphite mixture. The filament was then dried under a heating lamp, and introduced into the mass spectrometer.

One isotopic measurement run took approximately 8 minutes including base line measurement, and each analysis consisted of 50 scans. Ion beam intensities of m/z = 308 for 0.05 to 0.1 and 0.14 to 1 μg of B were more than $4 \times 10^{-13}$and 2×10^{-13} A, respectively. The filament current during the measurement was typically 1.0 to 1.2 A. The B isotopic compositions are expressed as a permil deviation (δ^{11}B) relative to NIST SRM951 boric acid:

$$\delta^{11}\mathrm{B}(‰) = ((^{11}\mathrm{B}/^{10}\mathrm{B})_{sample}/(^{11}\mathrm{B}/^{10}\mathrm{B})_{SRM951} - 1) \times 1000$$

We found that the determined ^{11}B/^{10}B ratio strongly depended on the sample size. Mean ^{11}B/^{10}B ratios and reproducibilities ($\pm 2\sigma$) of repeated SRM 951 analyses were 4.0517 ± 0.0011 (n=7), 4.0502 ± 0.0012 (n=5), and 4.0439 ± 0.0042 (n=5) for 1, 0.14, and 0.05 μg of B, respectively, corresponding to reproducibilities ($\pm 2\sigma$) of δ^{11}B of 0.27 ‰ 0.30 ‰ and 1.03 ‰ again respectively (Table 3). In order to avoid the mass fractionation during TIMS analyses related to the amount of B loaded, we used two different $(^{11}\mathrm{B}/^{10}\mathrm{B})_{SRM951}$ values for normalization of data for unknown samples (4.0517 for JB-2 and the glass vial; 4.0502 for 1C, 2C and PML-Allende).

Table 3: Boron sample size and ^{11}B/^{10}B ratios of NIST.

No.	^{11}B/^{10}B		$2\sigma_{mean}$
1mg of boron			
1	4.0527	±	0.0003
2	4.0519	±	0.0005
3	4.0513	±	0.0004
4	4.0512	±	0.0003
5	4.0511	±	0.0004
6	4.0517	±	0.0005
7	4.0516	±	0.0004
Average	4.0517	±	0.0011 (2σ)
0.14mg of boron			
1	4.0509	±	0.0007
2	4.0502	±	0.0005
3	4.0500	±	0.0003
4	4.0507	±	0.0006
5	4.0494	±	0.0006
Average	4.0502	±	0.0012 (2σ)
0.05 mg of boron			
1	4.0447	±	0.0024
2	4.0438	±	0.0023
3	4.0464	±	0.0028
4	4.0441	±	0.0023
5	4.0407	±	0.0024
Average	4.0439	±	0.0042 (2σ)

Reproducibility (2σ) of δ^{11}B for 1, 0.14, and 0.05 mg of B sample sizes is 0.27, 0.30, and 1.03 ‰, respectively.

Boron concentrations for reagents were determined by an isotope dilution method using TIMS by secondary electron multiplier (SEM) with a peak-jumping mode. The gain of the SEM against the FAR is set to be 120. Ion beam intensities of m/z = 308 for 40 ng B

were more than 4×10^{-15} A. The $^{11}B/^{10}B$ of the reagent and environmental blanks were also determined by the SEM peak-jumping mode. The mean and reproducibility (2σ) of SRM951 and SRM952 boric acid for 40-50 ng of B are 4.0513 ± 0.0169 and 0.0542 ± 0.0007 (n=5), respectively.

Lead The procedures for Pb analyses by TIMS were similar to those described by Kuritani & Nakamura (2002). Rhenium ribbon with thickness of 0.025 mm and width of 0.75 mm was formed into filaments. Trapezoid-shaped Re filaments (2 mm top × 0.025 mm thickness × 0.75 mm width) were used in this study. Prior to sample loading, the filaments were out-gassed for 30 min with a filament current of 4.5 A at 10^{-6} Torr. The Pb sample, dissolved in 1 μL of emitter consisting of silicic acid and diluted phosphoric acid (Gerstenberger & Haase, 1997), was loaded onto the top of the filament. The filament current was raised to 1 A, and held there until the drops on the filament disappeared. The current was kept at 1 A for another 30 seconds, and the current was abruptly decreased to zero. The sample was then introduced into the mass spectrometer.

Determinations of Pb isotopic composition were carried out using 5 Faraday cup collectors appropriately configured to collect ^{204}Pb, ^{205}Pb, ^{206}Pb, ^{207}Pb, and ^{208}Pb. The integration time for one ratio was 8 seconds. Idling and counting times for the baselines at 205.5 m/z were 8 and 16 seconds, respectively, and the baselines were measured after each block. One isotopic measurement run, consisting of 110 ratios in 10 blocks, took about 40 minutes including the gain calibration. Ion currents of ^{208}Pb are typically within the range of 3×10^{-11} to 6×10^{-11} A for loads of ~100 ng Pb (filament current of about 2 A) just before the start of the acquisition, at which point the temperature of the filament reaches 1230 ~ 1250°C. For samples with ~10 ng of Pb (sample 1C), ion currents are $1 \times 10^{-11} \sim 2 \times 10^{-11}$ A (filament current of 1.6–1.7 A) and the temperature of the filament is about 1100°C just prior to measurement.

Mass discrimination during the analysis was corrected by the method of "zero-time correction" (Tuttas & Habfast, 1982; Koide & Nakamura, 1990). The corrected data were then normalized using the correction factor determined by measured and recommended compositions of a Pb standard solution (NBS 981). Measured isotopic ratios of NBS 981 were $^{206}Pb/^{204}Pb$ = 16.8839 ± 0.0017, $^{207}Pb/^{204}Pb$ = 15.4187 ± 0.0023, and $^{208}Pb/^{204}Pb$ = 36.4685 ± 0.0069 (n=15, $\pm2\sigma$). The recommended composition of NBS981 by Todt *et al.* (1996) was followed. NBS 983 solution, which is enriched in ^{206}Pb, was used as a spike solution for isotopic dilution mass spectrometry to determine Pb blanks.

Lithium The mass spectrometric technique used in this study was essentially the same as that developed by Moriguti & Nakamura (1993). In this method Li^+ ion is ionized, using Li phosphate as an ion-source material, by a double filament method with Re filaments (0.025 mm thickness × 0.75 mm width). Prior to sample loading, filaments were outgassed for 30 minutes at a filament current of 4.5 A and a 10^{-6} Torr pressure. Afterwards, the distance between the sample and ionization filaments was adjusted to 1 mm, appropriate for the double-filament method. The purified Li sample was dissolved in 1 μL of 1D H_2O and then loaded at a point on the filament with a filament current of 0.9 A. The filament current was then slowly raised to 1.7 A and held there until the fume of phosphoric acid disappeared. The sample was then introduced into the mass spectrometer.

The analytical reproducibility for 100 ng of Li depends on the technique of sample loading onto the Re filament. The reproducibility for 100 ng Li with spread loading technique was 0.79 ‰ (RSD), which was two times larger than that for 250 to 1000 ng of Li (0.40 ‰

(Moriguti & Nakamura, 1998)). Moreover, the mean value from repeated analyses for 100 ng of Li using isotopic standard (NIST L-SVEC) was 2.2 ‰ lower than that for 250 to 1000 ng of Li (Moriguti & Nakamura, 1998). On the other hand, the analytical reproducibility for 100 ng Li with spot loading technique was 0.50 ‰ (12.1131 ± 0.0121 (2σ); n=8; Table 4). In the spot loading technique, furthermore, the mean value from 100 ng analysis is consistent with the value from 500 ng analysis within error (12.1067 ± 0.0070 (2σ); n=5) (Table 4). In this study, Li obtained through the entire chemical separation process is 100 to 500 ng (Table 7). Therefore, the spot loading technique was adopted in this study.

Table 4: Repeated analyses of the lithium isotopic composition of NIST LSVEC.

Sample size	No.	^{7}Li / ^{6}Li		$2\sigma_{mean}$
NIST LSVEC				
100 ng	1	12.1104	±	0.0007
	2	12.1169	±	0.0010
	3	12.1151	±	0.0006
	4	12.1130	±	0.0007
	5	12.1230	±	0.0007
	6	12.1018	±	0.0007
	7	12.1143	±	0.0006
	8	12.1106	±	0.0008
	Average	12.1131		
	2σ	0.0121		
	RSD (%)	0.050		
500 ng	1	12.1053	±	0.0006
	2	12.1057	±	0.0011
	3	12.1130	±	0.0010
	4	12.1046	±	0.0005
	5	12.1051	±	0.0005
	Average	12.1067		
	2σ	0.0070		
	RSD (%)	0.029		

In order to stabilize the magnetic field and accelerating voltage, the mass spectrometer was warmed up for more than 3 hours using the same acquisition condition as that used in the Li isotope analysis (described below). This warming technique makes peak jumping between m/z = 6 and 7 possible without fail. The ionization filament was heated to 1150°C, as measured by optical pyrometer, equivalent to a filament current of 1.55 to 1.65 A. The current in the filament with the sample was then raised rapidly to 0.3 A. The filaments were kept at this condition for 10 minutes. Then, both filament currents were immediately lowered to zero and the filaments were cooled for more than 10 minutes. Again, the ionization filament current was raised and fixed at 1.05 to 1.10 A, equivalent to a temperature of 850°C. The sample filament current was then increased slowly to 0.60–0.65 A, at which point the ^{7}Li signal appeared. After optimizing ion-beam focus, the sample filament current was instantaneously raised to 1.05 A and reduced to the current at which the ion-beam initially appeared. This operation was carried

out three times. After the ion-beam intensity stabilized, the current was raised slowly until the ion current of ^{7}Li reached 1.5×10^{-11} A (filament current of 0.70–0.78 A). It typically took about 20 minutes to attain a satisfactory ion current condition.

Data acquisition was done by peak jumping with a single Faraday cup collector using magnetic switching. The integration times for each mass peak and for the baseline were 4 and 16 seconds, respectively, and 55 ratios were collected in five blocks.

For NIST LSVEC, thirteen separate analyses of 100 to 500 ng of Li gave a mean ^{7}Li/^{6}Li ratio of 12.1107 ± 0.0120 (2σ). Li isotopic composition is expressed in the δ^{7}Li notation in parts in 10^{3} where:

$$\delta^{7}\mathrm{Li}(‰) = (({}^{7}\mathrm{Li}/{}^{6}\mathrm{Li})_{sample}/({}^{7}\mathrm{Li}/{}^{6}\mathrm{Li})_{NIST\ LSVEC} - 1) \times 1000.$$

An isotopic dilution method, using ^{6}Li-enriched CMNM-IRM015 (Joint Research Centre) as a spike, was used for the determination of the total procedural blank.

Strontium and rubidium

The mass spectrometric technique for Sr is essentially the same as that in Yoshikawa & Nakamura (1993). Trapezoid-shaped single W filaments (2 mm top × 0.025 mm thickness × 0.75 mm width) were used for Sr ionization in the ion-source of the mass spectrometer. Prior to sample loading, the W filaments were outgassed for 30 minutes at a filament current of 5.4 A and a 10^{-6}Torr pressure.

The separated Sr sample, dissolved with 1 μL of Ta-oxide solution (Yoshikawa & Nakamura, 1998), was loaded onto a Trapezoid-shaped W filament. The sample was dried at a filament current of 1.2A. Afterwards, the filament current was slowly raised to 2.5 A and heated to a dull red color at around 3.5 A. The loaded samples were then introduced into the mass spectrometer.

Determination of Sr isotopic composition was carried out using 5 Faraday cup collectors appropriately configured to collect ^{84}Sr, ^{85}Rb, ^{86}Sr, ^{87}Sr and ^{88}Sr. The isobaric interference of ^{87}Rb to ^{87}Sr was corrected by monitoring ^{85}Rb. The integration time for one ratio was 8 seconds. In Yoshikawa & Nakamura (1993), the baselines at 84.5, 85.5, 86.5, 87.5, and 88.5 m/z were measured after each block, which consists of 11 ratio acquisitions. In this study, based on the method of Yokoyama *et al.* (2001), the baseline measurements of Faraday cup collectors were carried out just before data acquisition in order to reduce data acquisition time. The analytical results obtained for NIST SRM 987 in this study were consistent with those in Yoshikawa & Nakamura (1998) within analytical reproducibility. Data acquisition was started when the ^{88}Sr ion current of 5×10^{-11} A (filament current of 3.7–3.9 A) was achieved. One isotopic measurement run consisted of 110 ratios in 10 blocks and took about 30 minutes including the gain calibration. The collected Sr isotopic data were normalized to ^{86}Sr/^{88}Sr = 0.1194. Five separate analyses of Sr standard reference material (NIST SRM 987) gave a mean ^{87}Sr/^{86}Sr = 0.710227 ± 0.000007 (2σ).

In the mass spectrometric technique for Rb, a quantitative analysis by a ID-TIMS, Ta-Re (evaporation-ionization) double-filament method was adopted. Prior to sample loading, Ta and Re filaments (0.025 mm thick × 0.75 mm wide) were outgassed for 30 minutes at a 10^{-6}Torr pressure and a filament current of 3.5 and 5.0 A, respectively. The dried Rb sample was dissolved with 1 μL of 0.4M HNO_3 and then loaded onto a Ta filament. The sample was then dried at a filament current of 1.0 A. Afterwards, the filament current was slowly heated to a dull red color at ~ 2.0 A. The loaded sample was then introduced into the mass spectrometer.

Rb measurement was accomplished by an ion counting method using peak jumping mode between ^{85}Rb and ^{87}Rb and a 85.5 m/z baseline with the secondary electron multiplier (SEM). The ionization filament current was increased without raising the sample filament current until the ion counts of ^{85}Rb reached more than 10000 cps (ionization filament current of 1.2–1.7 A), and then data acquisition was initiated. The integration times for each mass peak and for the baseline were 4 and 8 seconds, respectively, and 7 ratios were collected in 5 blocks.

The isobaric interference of ^{87}Sr with ^{87}Rb was negligible during data acquisition due to the large difference in ionization temperature between Rb and Sr. This difference in ionization temperature is enhanced by the Ta-emitter, loaded with the Sr fraction on the filament. The analytical reproducibility was better than 1% (2σ%, n = 10) for 1 pg of Rb.

Neodymium and samarium

The mass spectrometric technique for Nd isotope analysis is essentially the same as that in Makishima & Nakamura (1991b). A double filament method with Re filaments (0.025 mm thickness × 0.75 mm width) was adopted for Nd ionization. Prior to sample loading, Re filaments were outgassed for 30 minutes at a filament current of 5.0 A and a 10^{-6}Torr pressure.

The dried Nd sample was dissolved with 1 μL of 0.4M HNO_3 and then loaded onto a filament. The sample was dried at a filament current of 1.0 A. Then, the filament current was raised to produce a dull red color at around 2.0 A and maintained for 30 seconds. The loaded sample was then introduced into the mass spectrometer.

Determination of Nd isotopic composition was carried out using 5 Faraday cup collectors appropriately configured to collect ^{143}Nd, ^{144}Nd, ^{146}Nd, ^{147}Sm and ^{150}Nd. The isobaric interference of ^{144}Sm and ^{150}Sm with ^{144}Nd and ^{150}Nd, respectively, was corrected by monitoring ^{147}Sm. The integration time for one ratio, the method of baseline measurement, and the number of ratios and blocks in data acquisition were the same as those in the Sr isotope analyses in this study. The collected Nd isotopic data are normalized to ^{146}Nd/^{144}Nd = 0.7219. Eight separate analyses of Nd standard reference material (La Jolla) gave a mean ^{143}Nd/^{144}Nd = 0.511892 ± 0.000007 (2σ).

In the determinations of Sm concentration, the techniques for sample loading onto the Ta filaments and for the mass spectrometry were almost identical to those for the Rb quantitative analyses by ID-TIMS (see above). Samarium measurement was accomplished by ion counting methods using peak jumping mode between ^{147}Sm and ^{149}Sm and m/z = 147.5 baseline with the SEM. The ionization filament current was increased to 4.8 A and then the evaporation filament current was raised until the ion counts of ^{147}Sm exceeded 10000 cps (evaporation filament current of around 1.0 A) and then data acquisition was started. The analytical reproducibility was better than 1% (2σ%, n = 10) for 1 pg of Sm.

Results and discussion

Boron The measured δ^{11}B values of 1C, 2C, PML-Allende, JB-2, and borosilicate glass vial are listed in Table 5. Duplicated analyses of standard rock sample, JB-2, and PML-Allende were carried out in order to examine the analytical reproducibility for the natural rock samples. The amounts of B loaded on the filament were 1 μg for JB-2 and 0.078–0.087 μg for PML-Allende. The differences in the duplicated δ^{11}B values are 0.1 ‰ for JB-2 and 1.2 ‰ for PML-Allende with analytical precision ($2\sigma_{mean}$) for an individual analysis ranging from ± 0.1 ‰ to ± 0.3

Table 5: Boron isotopic compositions for the competition samples, JB-2, the PML-Allende samples, and the glass vial.

Sample	Sample size (mg)	$^{11}B/^{10}B$		$2\sigma_{mean}$	$\delta^{11}B$		$2\sigma_{mean}$
1C	0.138	4.0478	±	0.0008	-0.6	±	0.2
2C	0.147	4.0511	±	0.0012	0.2	±	0.3
JB2-1	2.00	4.0841	±	0.0005	8.0	±	0.1
JB2-2	2.00	4.0836	±	0.0005	7.9	±	0.1
Allende-1	0.087	4.0570	±	0.0013	1.7	±	0.3
Allende-2	0.078	4.0523	±	0.0021	0.5	±	0.5
Allende-3	0.165	4.0541	±	0.0006	0.9	±	0.2
Glass vial	8.00	4.0463	±	0.0003	-1.3	±	0.1
2C (0.147mg)-vial (0.075mg)		4.0564	±	0.0012	1.5	±	0.3

Sample size represents boron weight (mg) in sample powder for dissolution.
Only 1mg of boron is used for TIMS analyses of JB2 and the glass vial.

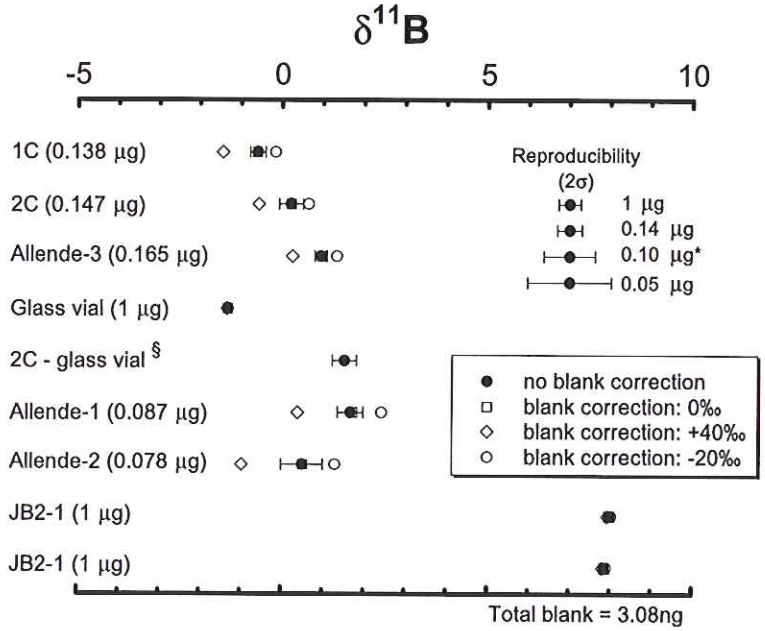

Fig. 7: $\delta^{11}B$ of the analyzed samples relative to SRM951. The error bars are $2\sigma_{mean}$ precision for each datum. The reference values after blank corrections, when the $\delta^{11}B$ of the blank is 0.40, and –20 ‰, are also plotted. The 2σ reproducibilities for each sample size are determined by 5 to 7 analyses of SRM951. § After the reduction of glass contamination calculated as 2C (0.147μg) minus glass vial (0.068 μg). * Reproducibility for 0.10 mg after Nakano & Nakamura (1998).

–0.5 ‰ respectively. This precision is well within the reproducibility for 1 μg and 0.05 μg or 0.1μg (± 0.63 ‰ Nakano & Nakamura, 1998) samples of B in the SRM 951 standard, again respectively.

The blank of the 1D H_2O and the total procedural blank for B were 10-20 pg mL^{-1} and 3.08 ng, respectively. The proportion of the B blank in the analyses of 1C and 2C is 2%. Although a

2% blank is not negligible, it is difficult to make the blank correction because of the difficulty in the determination of the $^{11}B/^{10}B$ for the procedural blank. The total procedural blank results from the reagents used and contamination from the environment. Boron isotopic fractionation would occur when the gaseous B in the environment is trapped into the liquid phase (^{10}B will be enriched in the liquid). When 50 mL of mix reagent (1D H_2O + HCl + HF), with approximately 5 μg of mannitol and 2 μg Cs, was left for two weeks and then evaporated, the obtained $\delta^{11}B$ of the blank was –98 to –113 suggesting isotopic fractionation of B with enrichment of ^{10}B relative to ^{11}B in the liquid. Therefore, only the reference $\delta^{11}B$ after blank correction with –20, 0, and 40 are plotted in the Fig. 7.

Because the competition sample powders were preserved in borosilicate glass vials containing approximately 4 wt.% of B, B contamination from the glass vial could be more serious than the procedural blank. The $\delta^{11}B$ of the glass vial is –1.3 ± 0.1 ‰ If 1C and 2C were contaminated from the glass vial, their actual $\delta^{11}B$ would be higher than the measured values depending on the amount of contamination. The major and trace element compositions and Sr, Nd, and Pb isotopic ratios of 2C are similar to those of PML-Allende (Table 1), and the B concentration of 2C (2.11 μg g^{-1}) is significantly higher than that of PML-Allende (1.14 μg g^{-1}). If 2C is assumed to be Allende chondrite, 0.068 μg of the 0.147 μg B came from the glass vial. The $\delta^{11}B$ obtained after the glass contamination correction is 1.5 ± 0.3 ‰ the same value as that for PML-Allende chondrite (1.0 ± 0.2 ‰, 0.165 μg of B) within error. Therefore, if 2C is Allende chondrite, data reveal that such a borosilicate glass is not an adequate material for the containers.

Lead The measured isotopic compositions of samples 1C and 2C, along with those of PML-Allende and JB-2, are provided in Table 6. The total procedural blank of Pb, including the B column chemistry procedure, was 102 pg. Thus, blank correction might not be necessary, considering that we measured 12 ng of Pb for 1C and 126 ng of Pb for 2C. The procedural blank of only the Pb column chemistry, including the second column procedure, was 34 pg, indicating that 2/3 of the total blank was derived from the B chemical separation procedure and the spike solution containing Rb, Sr, Nd and Sm.

The analytical reproducibility for Allende chondrite and JB-2 is somewhat wrong, resulting from unexpected mass discrimination during spectrometer analysis of the samples Allende-2 and JB-2-1. This could have been due to relatively large amounts of impurities such as organic materials in the separated Pb samples, which are believed to change the behavior of mass fractionation (Woodhead *et al.*, 1995). The Pb isotopic composition of Allende chondrite and JB-2 may, thus, be represented by the data for samples Allende-1 and JB-2-2. Improved analytical reproducibility might have been obtained if the second column chemistry was performed for samples Allende-2 and JB-2-1. In fact, for natural rock samples, we have now achieved analytical reproducibility of 0.011% (2σ) for $^{206}Pb/^{204}Pb$, 0.006% for $^{207}Pb/^{204}Pb$, and 0.020% for $^{208}Pb/^{204}Pb$, by performing the second column procedure even for samples with relatively large amounts of Pb (>50 ng) (Kuritani & Nakamura, 2002).

The measured compositions are shown in a plot of $^{207}Pb/^{204}Pb$ vs. $^{208}Pb/^{204}Pb$ (Fig. 8). The Pb isotope composition of sample 1C is highly evolved, and the $^{208}Pb/^{204}Pb$ ratio is close to 40. This evolved composition could have originated from marked enrichment of ^{206}Pb, ^{207}Pb, and ^{208}Pb due to radioactive decay of U and Th. The composition of sample 2C is not as evolved as that of 1C, and is close to the composition of PML-Allende.

Table 6: Summary of lead isotopic compositions of the competition samples, along with those of PML-Allende chondrite and GSJ JB-2

	$^{208}Pb/^{204}Pb$	$^{207}Pb/^{204}Pb$	$^{206}Pb/^{204}Pb$
1C	39.8170	16.4861	20.0022
2C	36.1099	14.0605	16.3639
Allende-1	35.9009	14.0654	15.9150
Allende-2	35.8783	14.0484	15.8786
JB2-1	38.2793	15.5602	18.3438
JB2-2	38.2511	15.5524	18.3324
Total Procedural Blank (n=2, 1σ)			102 ± 24 (pg)
Procedural Blank for Pb Column			34 ± 2 (pg)

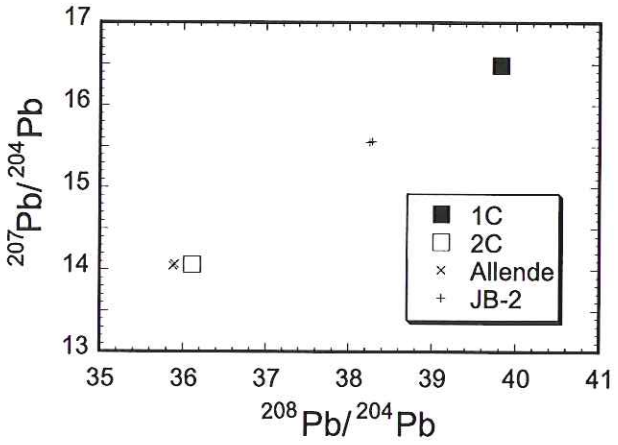

Fig. 8: Lead isotope compositions of the competition samples 1C and 2C, along with those of PML-Allende and GSJ JB-2.

Lithium Sample sizes of analyzed samples, Li contents obtained by ICP-MS, estimated amounts of Li for the TIMS analyses, measured Li isotopic compositions, in-run precision ($2\sigma_{mean}$) for each analysis and total procedural blank are shown in Table 7. We obtained a total procedural Li blank of 17 pg. Although this value was about 1.5 times larger than that (11 pg) from Li-single separation procedure (Moriguti & Nakamura, 1998), it is not necessary to carry out blank collection for the analyses in this study using more than 100 ng of Li. 1C and 2C have similar δ^7Li values, +6.3 and +5.1 ‰ respectively. The average of two δ^7Li values for JB-2 is +3.3 ‰. This value is 1.3 ‰ lower than that in Moriguti & Nakamura (1998) (+4.9 ± 0.8 ‰ (2σ)). Furthermore, duplicate analyses of PML-Allende (+5.6 and +6.7 ‰) are 2.2 to 3.3 ‰ lower than the value (+8.9 ‰: unpublished data) obtained through an independent Li separation procedure. Because the Li blank is negligible in this study, these systematic differences

Table 7: Weights of sample, Li concentrations, amounts of Li and analyzed Li isotopic compositions.

Sample	Sample (mg)	Li (μg g^{-1})	Li (ng)	δ^7Li (‰)	$2\sigma_{mean}$
1C	69.1	2.00	138	6.30	0.10
2C	70.1	1.70	119	5.14	0.06
Allende-1	76.2	1.60	122	6.67	0.05
Allende-2	68.4	1.60	109	5.63	0.19
JB2-1	63.8	8.04	513	3.33	0.05
JB2-2	62.8	8.04	505	3.27	0.09

Total procedural blank for Li = 17 pg

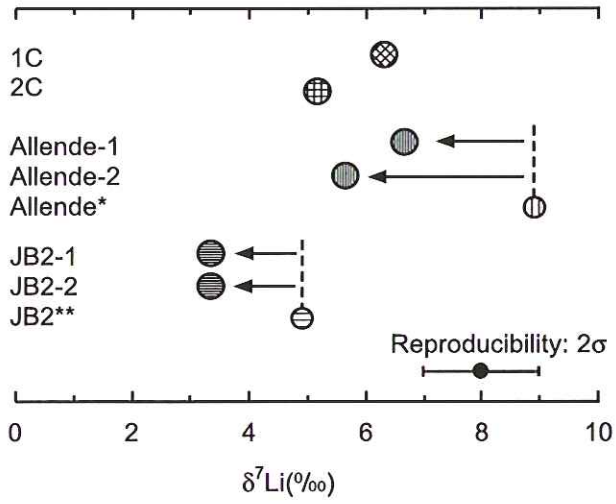

Fig. 9: Li isotopic compositions of the analyzed samples. Error bar represents reproducibility (2σ) from spot loading technique of 100 to 500 ng of Li using NIST LSVEC. Arrows mean that obtained data from integrated chemical separation method in this study are lower than those from the separation method of Moriguti & Nakamura (1998). * unpublished data. ** data from Moriguti & Nakamura (1998). * and ** Li separation was carried out by the separation method of Moriguti & Nakamura (1998).

of δ^7Li value cannot be caused by blanks. After our Li isotope analyses, we discovered that a very small amount of Li was eluted before collection of a fraction including Pb, Li, Rb, Sr, Sm and Nd in the first column of the B separation process. A ^{7}Li-enriched fraction is eluted at the beginning of the Li fraction in cation exchange chemistry using HCl as an effluent (Moriguti & Nakamura, 1998). Therefore, these systematic differences (demonstrated on Fig. 9) may be caused by the loss of Li in the ion-exchange chemistry. Thus, the actual δ^7Li values of 1C and 2C may be $1 \sim 3$ ‰ higher than the values obtained in this study. In order to overcome this problem, Li should be collected before collection of the B fraction at the second column stage of the B separation procedure.

Strontium, rubidium, neodymium and samarium Analytical results for 1C, 2C, PML-Allende and JB-2 are provided in Table 8. Rb-Sr and Sm-Nd isotope plots are presented in Figs. 10 and 11. Rb, Sr, Sm and Nd data for 1C-O and 2C-O are collected after B, Pb and Li chemical separations using approximately 70 mg of each sample. Total procedural blanks for Rb, Sr, Sm and Nd were 6, 134, 2 and 14 pg, and are considered to be negligible for these two samples.

Table 8: Rb, Sr, Sm and Nd isotope compositions of the competition samples, PML-Allende and JB-2.

		concentration (μg g^{-1})		total amount (ng)					
sample	fraction*	Rb	Sr	Rb	Sr	$^{87}Rb/^{86}Sr$	$^{87}Sr/^{86}Sr$		$2\sigma_{mean}$
1C	O	3.84	11.8	265	817	0.943	0.759853	±	8
	A	4.01	11.0	(<40)	(<110)	1.06	0.760609	±	16
	B	-	-	(<40)	(<110)		0.759561	±	16
2C	O	1.17	14.9	81.9	1045	0.227	0.713926	±	11
	A	1.27	13.4	(<13)	(<130)	0.275	0.714028	±	13
	B	-	-	(<13)	(<130)		0.714328	±	15
Allende 1		1.31	14.4	100	1101	0.263	0.716538	±	9
Allende 2		1.31	14.4	89.6	987	0.263	0.716523	±	8
JB2-1		6.53	189	416	12047	0.216	0.703648	±	8
JB2-2		6.21	178	390	11164	0.217	0.703647	±	7
total blank	(pg)	6	134						

		concentration (μg g^{-1})		total amount (ng)					
sample	fraction*	Sm	Nd	Sm	Nd	$^{147}Sm/^{144}Nd$	$^{143}Nd/^{144}Nd$		$2\sigma_{mean}$
1C	O	0.212	0.651	14.7	45.0	0.197	0.512696	±	8
	A	0.164	0.560	(<1.6)	(<5.6)	0.177	0.512803	±	18
	B	-	-	(<1.6)	(<5.6)		0.512997	±	55
2C	O	0.324	1.01	22.7	70.7	0.194	0.512608	±	6
	A	0.323	1.00	(<3.2)	(<10)	0.196	0.512599	±	21
	B	-	-	(<3.2)	(<10)		0.512599	±	15
Allende 1		0.324	1.00	24.7	76.1	0.196	0.512654	±	4
Allende 2		0.323	1.00	22.1	68.2	0.196	0.512634	±	7
JB2-1		2.42	6.78	154	432	0.216	0.513154	±	5
JB2-2		2.23	6.23	140	391	0.217	0.513144	±	6
total blank	(pg)	2	14						

* Fraction O was collected after B, Pb and Li separation. A and B were collected after trace element analyses and HFSE analyses using the ICP-MS.

In addition to the above samples, we analyzed the Sr and Nd isotopic compositions in samples 1C-A, 1C-B, 2C-A, 2C-B (Table 8), using the remaining sample solutions that were used for trace element analyses using ICP-MS (Group-I and –II, see Section 2.2). The sample amount used in these analyses corresponded to $\sim$ 5 mg because almost half of the 10 mg sample had been used in the previous analyses of the ICP-MS. Chemical separation procedures applied to these samples are the same as those described in Chapter 3, and the procedural total blanks of Rb, Sr, Sm and Nd are essentially identical to those for individual chondrule analyses (0.7, 20, 0.4 and 2 pg, respectively). Blank corrections were not also carried out to these samples because such small blanks would not affect the isotope results.

Sample 1C The Sr and Nd isotopic compositions of samples 1C-O, -A and -B are significantly different with the differences exceeding the analytical errors. Also the $^{87}Rb/^{86}Sr$ and $^{147}Sm/^{144}Nd$ ratios do not agree for 1C-O and -A. These observations, and a consideration of the sample sizes used for 1C-O, -A and –B, indicate that 1C was heterogeneous in terms of both concentration and isotopic compositions. A Rb-Sr isotope plot is presented in Fig.

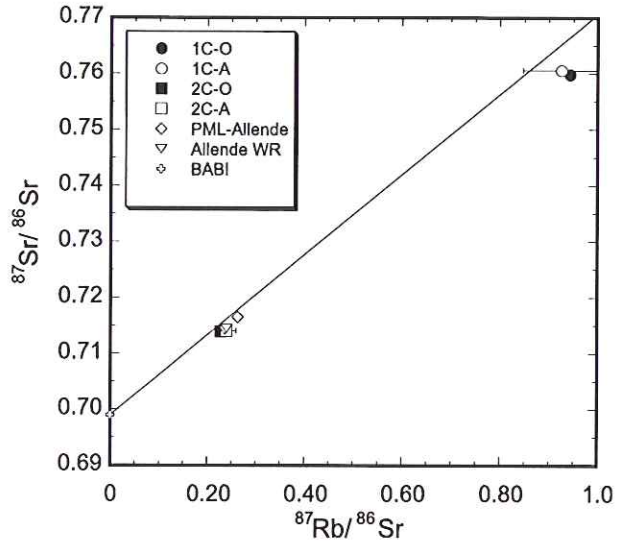

Fig. 10: Rb-Sr diagram for the competition samples. Solid line is the 4.56 Gy model line. BABI (basaltic achondrite best initial, $^{87}Sr/^{86}Sr = 0.69899 \pm 0.000047$) is from Papanastassiou & Wasserburg (1969). Allende WR is Allende whole rock data from Tatsumoto *et al.* (1975).

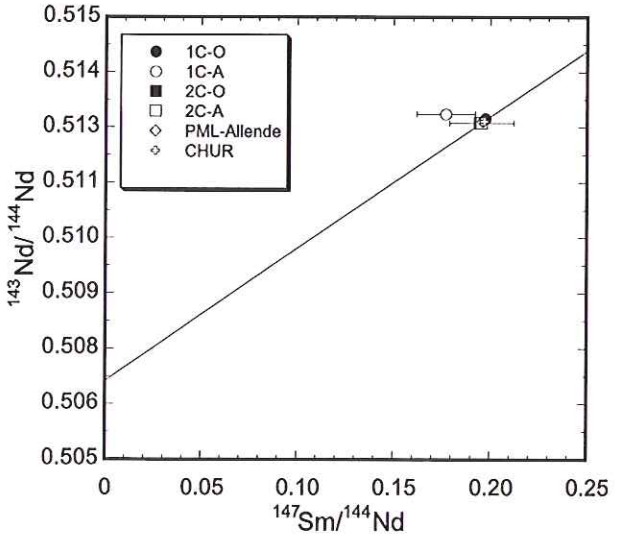

Fig. 11: Sm-Nd diagram for the competition samples. Solid line is the 4.56 Gy model line. CHUR (chondritic uniform reservoir, $^{147}Sm/^{144}Nd = 0.1967$ and $^{143}Nm/^{144}Nd = 0.512638$) is from DePaolo & Wasserburg (1976).

10. The Sr isochron age calculated from 1C-O, -A and BABI (basaltic achondrite best initial) (Papanastassiou & Wasserburg, 1969) is 4.405 ± 0.004 Ga (MSWD = 0.56). In the Sm-Nd plot (Fig. 11), the variations of both the isotopic compositions of Nd and the Sm/Nd ratios are too small to calculate an isochron age, although they do plot near a 4.56 Ga model line for the chondritic uniform reservoir (CHUR) (DePaolo & Wasserburg, 1979).

Sample 2C

The Sr isotopic compositions and $^{87}Rb/^{86}Sr$ ratios are also significantly different among samples 2C-O, -A and –B. In contrast, the Nd isotopic compositions and $^{147}Sm/^{144}Nd$ ratios of the three samples are identical (within the analytical errors), and very close to those of the PML-Allende. The Rb-Sr isotope diagram for 2C-O, -A and BABI (Fig. 10) gives an apparent isochron age of 4.484 ± 0.012 Ga (MSWD = 1.12). These observations indicate that the powdered sample, 2C, was homogeneous in terms of trace element and isotopic compositions, and very similar to the PML-Allende. This is also supported by the results of other trace elements and isotopic compositions as given in the previous sections.

PML-Allende and JB-2

The duplicated analyses of PML-Allende and JB-2 are consistent in Sr and Nd isotopic compositions, and $^{87}Rb/^{86}Sr$ and $^{147}Sm/^{144}Nd$ ratios. Furthermore, Rb, Sr, Sm and Nd concentrations obtained for PML-Allende by ID-TIMS are almost identical in the duplicated analyses (Table 8). However, the duplicated analyses of element concentrations are significantly different for JB-2; i.e., the results for JB-2-1 are 5–9% higher than those of JB-2-2 and the JB-2-1 values agree with the reference values given in Table 1. Such a disagreement might be derived from an accidental loss of spikes during evaporation of the spike solution from the Teflon beaker undertaken to reduce the B blank in the spike solution prior to sample weighing (see Section 2.3). If we lose some spike from the beaker, perhaps due to static electricity on the Teflon, this results in concentrations higher than the correct values. However, the element abundance ratios do not change because a part of the spike, in fluoride-form after evaporation with HF solution might have flown out of the Teflon beaker as a small flake. Consequently, about 5% of the spike (by weight) might have been lost according to the results for JB-2-2. In order to prevent such loss of spike during evaporation to dryness in the Teflon beaker, the addition of tiny amounts of phosphoric acid solution might prove useful, as phosphoric acid can not be evaporated at 100°C and does not interfere with the following chemical separation procedure for B.

2.4 Re-Os isotope systematics

Analytical procedure

Because the analytical procedure for Re and Os determinations is described in Section 2.2, only the Os isotope determination is described here. After the ion exchange chemistry for separation of PGE after Makishima *et al.*,(2001), Os was further purified by microdistillation developed by Birck *et al.* (1997). $^{187}Os/^{188}Os$ ratios were determined as OsO_3^- ion by negative thermal ionization mass spectrometry (N-TIMS) employing a Finnigan MAT262 (nicknamed "SARU"). A single peak-jumping method was applied with 110 scans in one run using RPQ-SEM. $^{190}Os/^{188}Os$=1.9879 was used for normalizing the obtained $^{187}Os/^{188}Os$ ratios. Precision in one run is calculated as $2\sigma_{mean}$. Reproducibility of the $^{187}Os/^{188}Os$ ratio, determined using an in-house Os standard of 0.5 pg, was 1% (2σ). Details of the mass spectrometry will be presented in Makishima & Nakamura (in prep.) Because the total blank was 2 pg and negligible, no blank correction was performed for the isotope ratio calculations.

Results and discussions

Re and Os concentrations, $^{187}Os/^{188}Os$, and $^{187}Re/^{188}Os$ ratios of the competition samples, together with those of the averages of quadruplicated Smithsonian-Allende analyses, are shown

Table 9: Re-Os isotope data for the competition samples.

	Re (ng g^{-1})	Os (ng g^{-1})	$^{187}Re/^{187}Os$	$^{187}Os/^{188}Os$	$2\sigma_{mean}$	Actual Re (ng)	Actual Os (ng)	Re blank (ng)	Os blank (ng)
1C	15.0	275	0.247	0.11950	0.00016	0.125	2.29	0.008	0.002
2C	70.3	631	0.479	0.12662	0.00012	0.657	5.89		
Average of Smithsonian Allende (n=4; 0.0083-0.016 g)					2σ				
	80.5	796	0.477	0.12621	0.00022	0.7-1.3	7-13		
Reference lines									
Initial			0	0.09563[a)]					
4.56 Ga			0.5	0.13166[b)]					
4 Ga			0.5	0.12738[b)]					

a) Shen et al., 1996.
b) λ_{Re}=1.64×10^{-11}y^{-1} (Lindner *et al.*, 1989.)

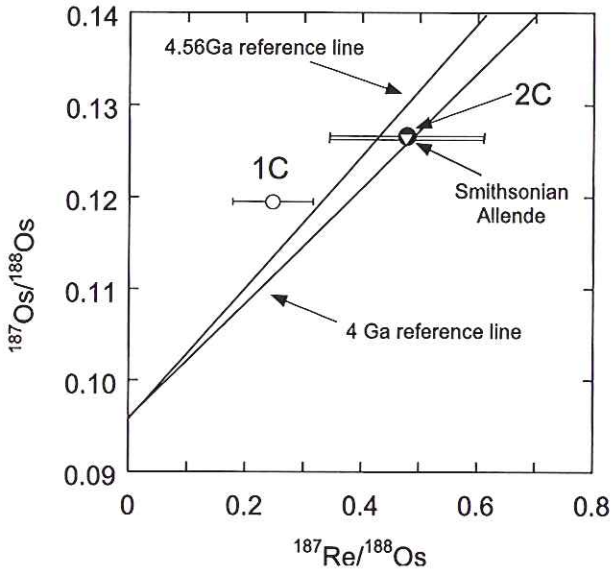

Fig. 12: Re-Os isochron plot fot the competition samples. Data for the average of Smithsonian-Allende ($n = 4$; open triangle) are also shown in the figure. The two lines are reference lines at 4.56 Ga and 4 Ga, shown in Table 9. The horizontal error bar shows uncertainty of 2σ. The vertical error (2σ) falls within the data point.

in Table 9. The actual Re and Os amounts in the competition sample aliquots and the total Re and Os blanks are also shown in Table 9.

Reproducibilities for Re and Os abundance in Smithsonian-Allende ($n = 4$), using 8.3–16 mg and analyzing by ICP-MS, were 9.8% and 12% (1σ), respectively. These errors were assumed to represent the maximum uncertainty of the competition samples, because the reproducibility of the Smithsonian-Allende analysis is affected by sample heterogeneity. The reproducibility of

the simultaneous Os isotope analysis by N-TIMS was 0.18 % (2σ). This is smaller than that of the Os standard analysis of 1%, so that the maximum uncertainty of $^{187}Os/^{188}Os$ for the competition samples is estimated to be 1%.

The analytical results are summarized on an isochron plot in Fig. 12. Error bars are plotted based on the maximum uncertainties discussed above. For comparison, 4.56 Ga and 4 Ga reference lines are also drawn in Fig. 12, depicting the calculatied values in Table 9. It is noteworthy that, on this plot, 2C samples are identical to the average of the Smithsonian-Allende powder, showing an age younger than 4.56 Ga. In contrast, 1C is plots above the 4.56 Ga isochron.

3. GEOCHEMICAL ANALYSES OF FRAGMENT SAMPLES (additional demonstration)

3.1 General sample preparation for the fragments

An overall flowchart of the analytical procedure for the fragment sample is presented in Fig. 13. Chondrules were separated mechanically from coarsely crushed PML-Allende meteorite using ceramic and stainless steel tools. Each separated chondrule was mounted with thermoplastic wax, Crystal bond, on a silicon wafer, and was sliced into 3 pieces using an automatic dicing saw, DAD522 (Disco ES Ltd.). Photographs of the typical slicing procedure are displayed in Fig. 14 and the slicing conditions are given in Table 10. The sliced pieces were carefully removed from the silicon wafer on a hot plate at a temperature of approximately 100°C, then the remaining wax was washed off using acetone. The center part was used to prepare a polished thin section for petrographic observations and probe analyses using an optical microscope, the SEM-EDX and an ion microprobe, and the two outer portions were used for the determinations of bulk trace element and isotopic compositions by ICP-MS and TIMS, respectively.

Table 10: Physical parameters for the slicing of the chondrule.

Sample	Blade type †	Chondrule diameter (mm)	Thickness of the sliced center part ‡ (μm)	Sample weight for the both side of slices †† (mg)
Ch9	B	1.6	210	1.665
Ch69	A	1.3	140	1.036
Ch145	A	0.97	70	0.353
Ch159	A	1.8	250	2.454
Ch162	A	2.0	100	1.024

† Blade A : 68 × 40 × 0.15 mm (outer ϕ , inner ϕ , and thichness of blade), Blade B : 66 × 40 × 0.07 mm
‡ Samples for the analyses by SEM-EDX and ion microprobe
†† Samples for ICP-MS and TIMS analyses

3.2 Major and trace element abundance of the fragments by probe analyses

The textural and petrographic observations were carried out using an optical microscope and a SEM-EDX unit (HITACHI S-3100H with HORIBA EMAX-7000). Major element compositions were determined using the SEM-EDX operated at 20 kV accelerating voltage and a 0.3 nA beam current. The major element compositions were corrected by the standard-less ZAF correction method of the EMAX-7000 program (HORIBA Ltd., Ver. 1.32). The analytical

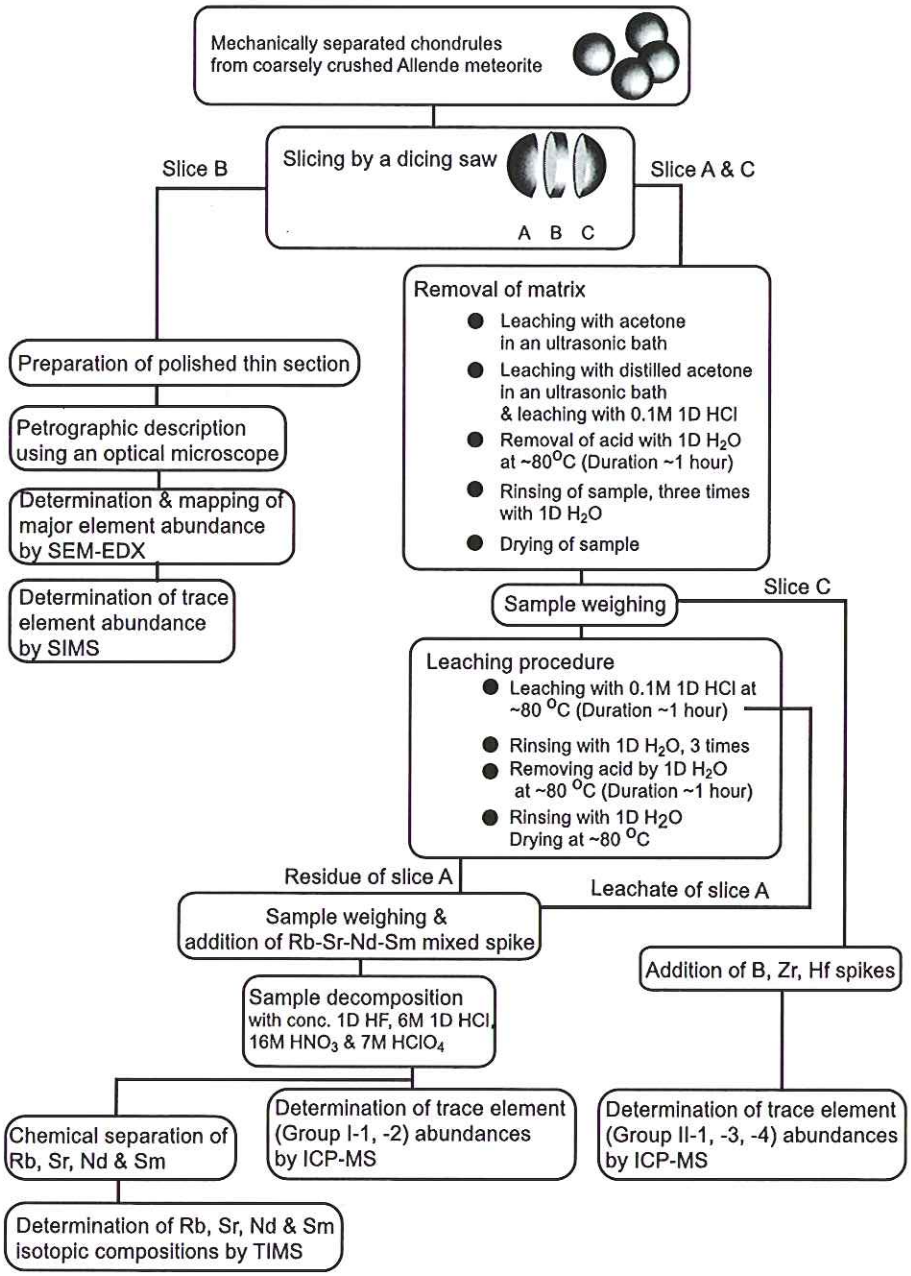

Fig. 13: Analitical flow chart for fragments of Allende chondrule.

points on the thin sections were recorded using a Visual Stage system, which was developed to support the probe analyses using the SEM-EDX and SIMS with extremely high spatial resolution. This provides identical spatial coordinates on images including reflected-light, plane-light and crossed-polarized optical images, SEM, BSE (back scattered electron), and compositional images from the SEM-EDX, and secondary ion image from the ion microprobes (Cameca ims-5f and -1270). This system made the analytical points easily and precisely (and repeatedly) accessible with extremely high precision in the positioning within 5 μm. This capability is

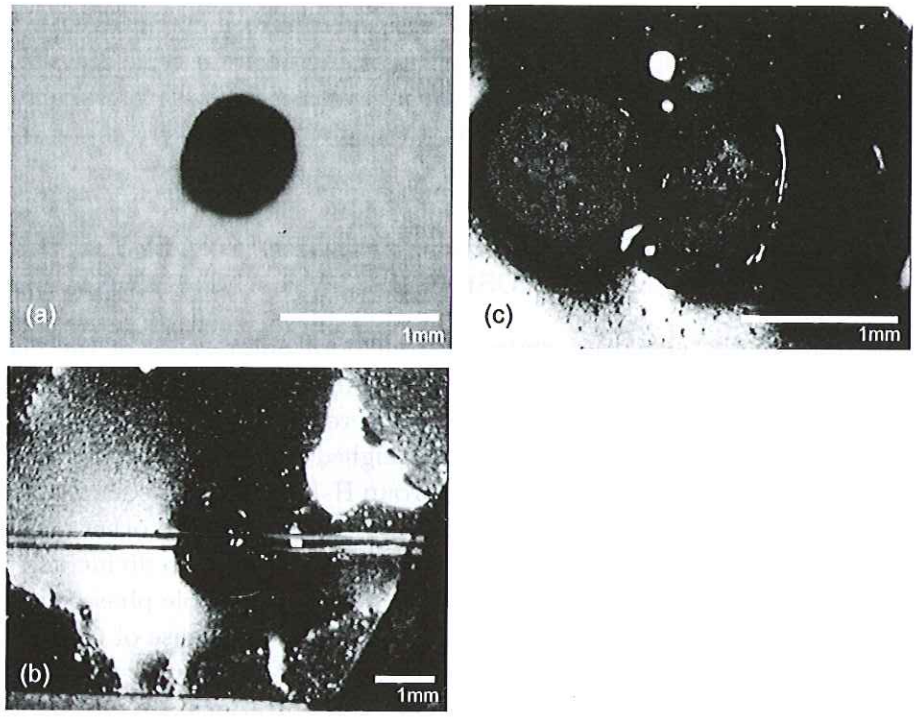

Fig. 14: Photographs of the slicing procedure, (a) typical chondrule, (b) chondrule after slicing and (c) chondrule slices removed from the thermoplastic wax.

indispensable especially for the trace element and isotope analyses using the ion microprobe, because the reflected-light optical image for analytical positioning is extremely poor.

Trace element analyses of clinopyroxenes, enstatite, olivine, plagioclase, nepheline, mesostasis, altered parts and melt inclusions, which were main components of Allende chondrule, were carried out employing the Cameca ims-5f ion microprobe at PML, Misasa, following the procedures described in Nakamura & Kushiro (1998). Standard materials used for the calibration of trace element concentrations were clinopyroxene from mantle xenoliths and basaltic glasses. These standards have been well characterized in terms of homogeneity and concentrations by both the ion microprobe and ICP-MS. In order to reduce the charging effect, the polished thin sections were coated by gold of 20 nm thickness.

The target materials on the thin section of the chondrule were sputtered with a highly focused O^- primary beam, which was accelerated by 12.5 kV resulting in approximately $5 \sim 10$ nA primary beam intensity with $5 \sim 10$ μm spot size. An energy filtering method (Shimizu & Hart, 1982) was applied to reduce the matrix effect to the secondary ions. Positive secondary ions were collected by ion counting using an energy offset of –45 to –60 V from 4500 V acceleration with an energy bandpass of ± 10 V. Even if an energy filtering is applied to the REE analysis, it is difficult to properly eliminate the isobaric mass interference of oxide ions of in particular, $^{135}Ba^{16}O$, $^{141}Pr^{16}O$ and $^{147}Sm^{16}O$ to ^{151}Eu, ^{157}Gd and ^{163}Dy, respectively. Therefore, correction factors to subtract the isobaric oxide interference were obtained empirically by measuring oxide/metal ion ratios in synthetic standard glasses (Nakamura & Kushiro, 1998, in detail).

These operational conditions resulted in $1 \sim 4 \times 10^5$ cps for ^{30}Si secondary ion during the

runs in which trace elements were analyzed. Analytical reproducibilities (RSD 1σ% in n = 10) for trace elements in the clinopyroxene and basaltic standard were typically ~5%, except for Ba (30%). The trace element abundances in the analyzed materials were similar to those in standard materials within an order of magnitude; therefore, analytical errors could be estimated to be ~10% to a few%.

4. BULK TRACE ELEMENT AND ISOTOPE ANALYSES OF THE FRAGMENTS USING ICP-MS AND TIMS

In order to remove the chondrite matrices from both outer slices of the chondrule, the slices were leached with distilled acetone for 1 hour and subsequently with 0.1M 1D HCl for 15 minutes in an ultrasonic bath. Leached samples were evaporated to dryness at 80°C after rinsing with 1D H_2O. Then, one of the slices was weighed and decomposed with B, Zr and Hf spikes for the determinations of trace elements (Group II-1, -3, -4). The details of the chemical procedures for the ICP-MS analyses are provided in Section 2.2. The other slice was leached again with 0.1M 1D HCl for 1 hour on a hot plate at 80°C, in order to divide it into a leachate and a residue corresponding to the acid-soluble and the acid-insoluble phases. It is difficult to separate the mineral phases mechanically in Allende chondrule because of the extremely small grain size of the constituent materials. We, therefore, decided to apply acid leaching, which is useful in examining the variation of trace element concentrations and isotope compositions in a single grain of chondrule due to the contributions of different phases. After the leaching, the solid residue separates were weighed and decomposed with one of the Rb-Sr-Nd-Sm mixed spikes (M2 or M3 in Table 2), which were also used for the isotope analyses of the powdered samples (see Section 2.3). The decomposed sample solution was split into two aliquots for trace element analyses (Group I-1, -2) using ICP-MS and for Rb, Sr, Sm and Nd isotope analyses using TIMS. Sample weight in each aliquot was calculated based on the weight ratio of these two aliquots and an original weight of the residue. The details of chemical and analytical procedure for the ICP-MS are described in Section 2.2.

In order to determine the isotopic compositions of aliquots with extremely small amounts of the elements concerned (Table 18), it is important to reduce the procedural blank. For this purpose, Sr-Rb and Sm-Nd fractions were collected by using a half volume of ion-exchange resin compared with the separation for the powdered samples in Section 2.3. 0.5 mL of Muromac AG 50WX12 resin was charged into a polypropylene column and the resin bed was successively cleaned by same method in Section 2.3 and conditioned with 0.5 mL of 4M HCl. The split sample solution was dried in the closed-system evaporator and dissolved in 0.5 mL of 4M HCl solution, then loaded onto the resin bed column. 1 mL of 2.8M HCl was added to the column and the mixed fraction of Rb and Sr was collected by 4 mL of 2.8M HCl. After that, the mixed fraction of Nd and Sm was collected by the subsequent addition of 4.5 mL of 6M HCl. These fractions were evaporated to dryness in the closed-system evaporator.

In order to purify Rb and Sr, the column used for the rough separations of Rb, Sr, Sm and Nd was again cleaned by same method in Section 2.3 and the resin was conditioned with 0.5 mL of 25% pyridine. The dried Sr-Rb mixed fraction was converted to pyridinium chloride by adding 0.03 mL of 25% pyridine and dried at 60°C, then dissolved in 2 mL of D.P.E.. This solution was loaded onto the column. 2 mL D.P.E., 4 mL of H_2O and 0.5 mL of 1.5M HCl were then successively added to the column to remove Mg, Ca and pyridine. The Rb fraction was collected with 1.5 mL of 2.8M HCl. Sr was finally eluted by 2 mL of 6M HCl after washing the column with 4 mL of 4M HCl. The Rb and Sr fractions were evaporated to dryness in the

Table 11: Mineral assemblages in the analyzed chondrules.

Name	Type†	olivine	diopside	enstatite	Other minor minerals (and melt inclusions)
Ch9	POP	+++	+	+	melt inclusions, nepheline, altered parts, Fe-olivine, spinel inclusion, opaques
Ch69	POP	++	+	+	Low-Ca cpx, plagioclase, nepheline, apatite, Fe-olivine, spinel inclusion, opaques
Ch145	POP	++	+	+	mesostasis, Low-Ca cpx, plagioclase, apatite, opaques
Ch159	-	+++	+	++	mesostasis, nepheline, plagioclase, Low-Ca cpx, apatite, opaques
Ch162	PO	++++	+	+	melt inclusions, mesostasis, altered parts, plagioclase, Low-Ca cpx, opaques, sulfide

† POP : Porphyritc olivine and pyroxene, PO : Porphyritic olivine

closed-system evaporator.

The purification technique for Sm and Nd was exactly the same as the procedure applied for the powdered samples in Section. 2.3.

4.1 Results and discussions

In this section, we present only the results obtained during the period of the analytical competition; we do not intend to interpret the results for understanding the formation and evolution of the chondrules and Allende meteorite, as this exercise is intended as a demonstration of our analytical capabilities for extremely small fragments.

The mineral assemblages of five chondrules separated from the Allende meteorite, identified using an optical microscope and a SEM-EDX, are summarized in Table 11. 30 elements were measured for constituent minerals, melt inclusions, mesostasis and altered parts in these chondrules by a combination of SEM-EDX and ion microprobe analyses. These results are compiled in Table 12-16, and are also displayed, as CI-chondrite normalized REE and trace element patterns and BSE and Al-Ca-Na mapping images, in Figs. 15-19.

24 trace elements in the bulk chondrules were determined by ICP-MS, and are given in Table 17. Extremely small amounts of the chondrules, ranging from 0.03 to 2 mg, were used for the ICP-MS analyses. In such low-concentration analyses, therefore, blank corrections are crucial for the extremely trace elements in the chondrules, as presented also in Table 17. CI-normalized element abundance patterns of the chondrules are shown in Fig. 20. As is clear in Fig. 20, the trace element characteristics of the chondrules are extremely uniform, showing flat patterns with strong Cs, Rb and B depletions relative to the adjacent elements, although actual abundances vary by a factor of 2. These patterns for the chondrules are essentially identical to those obtained for the PML-Allende powders in this study (see Fig. 4). These observations indicate that the sample preparation and analytical techniques established at PML using ICP-MS with flow-injection for very small sample sizes were extremely effective in the trace element analyses. In Table 17 and Fig. 20, the concentrations of Pb are preferable values because peculiar peak shapes for Pb, slightly different from that for the standard solution, were observed in the analyses by ICP-MS. Even in the trace element analyses by ICP-MS for common terrestrial samples such as volcanic rocks, this strange peak shape for Pb was observed when the elimination of fluorides formed during sample decomposition was imperfect. Therefore, we believe that Mg-fluorides remaining in the solution caused the strange peak shape of Pb in the ICP-MS; the chondrules have high Mg contents and we have noted that it sometimes difficult to completely decompose fluorides (Yokoyama *et al.*, 1999)

Aliquots of the sample solutions used for trace element analyses by ICP-MS were also used for the determinations of Rb, Sr, Nd and Sm isotope analyses by TIMS. These results,

Table 12: Major and trace element abundances in Ch9 determined by the SEM-EDX and the ion microprobe.

	Ch9-1-18 Oliv.	Ch9-1-20 Oliv.	Ch9-2-1 Melt Inc.	Ch9-2-3 Diop.	Ch9-3-6 Alt.(Neph.)	Ch9-4-1 Diop.	Ch9-4-2 Diop.	Ch9-4-8 Enst.	Ch9-5-2 Diop.	Ch9-5-7 Oliv.	Ch9-7-6 Alt.
(Wt. %)											
SiO_2	40.77	41.35	46.08	49.21	37.25	48.91	49.49	54.87	49.5	40.93	29.00
TiO_2	n.d.	n.d.	2.22	0.96	0.24	1.25	0.79	0.61	1.17	0.06	0.56
Al_2O_3	0.3	0.07	25.67	10.69	28.71	10.9	10.69	4.87	10.34	0.24	16.96
Cr_2O_3	0.11	0.03	0.34	1.00	0.43	1.09	1.16	0.98	1.08	0.12	0.17
MgO	53.97	54.31	3.43	17.51	4.03	18.12	18.34	35.36	17.65	55.94	31.41
MnO	0.04	0.03	0.06	0.15	0.07	0.28	0.23	0.17	0.2	n.d.	0.15
FeO	3.82	3.71	0.49	0.44	2.21	0.32	0.35	0.54	0.36	1.79	17.86
CaO	0.41	0.24	20.85	19.3	1.23	18.38	18.6	2.02	19.31	0.41	0.47
NiO	0.01	0.03	0.14	0.18	0.05	0.02	0.13	0.1	0.22	0.03	0.38
Na_2O	0.36	0.23	0.45	0.31	20.25	0.25	0.11	0.24	0.1	0.36	1.16
K_2O	0.01	n.d.	n.d.	0.01	0.12	0.04	n.d.	n.d.	n.d.	0.02	n.d.
P_2O_5	0.09	n.d.	0.15	0.20	0.13	0.24	0.09	0.06	n.d.	n.d.	0.18
SO_3	0.07	n.d.	0.1	n.d.	0.05	0.16	n.d.	0.16	0.07	0.09	1.69
Cl	0.03	n.d.	0.01	0.02	5.24	0.04	0.01	n.d.	n.d.	n.d.	0.02
Total	100	100	100	100	100	100	100	100	100	100	100
($\mu g\ g^{-1}$)											
Sr	0.743	0.090	86.8	5.84	52.9	6.32	7.29	1.39	7.42	0.045	15.8
Y	0.288	0.096	26.8	22.8	29.6	27.0	31.5	3.61	27.8	0.208	18.6
Zr	0.339	0.017	56.4	29.1	83.8	35.3	36.7	2.64	34.7	0.037	55.7
Nb	0.001	n.d.	3.86	0.036	4.98	0.041	0.039	0.009	0.042	n.d.	0.178
Ba	0.142	n.d.	18.3	0.253	107	2.42	0.717	0.168	1.18	0.051	5.78
La	0.021	0.002	3.98	0.777	6.17	0.596	0.619	0.145	0.864	n.d.	3.97
Ce	0.043	0.004	11.8	2.84	17.1	3.05	3.29	0.294	3.04	0.001	9.71
Pr	0.006	0.002	1.57	0.500	2.36	0.639	0.638	0.055	0.568	0.002	1.48
Nd	0.038	n.d.	7.93	3.84	11.5	4.29	4.80	0.370	4.43	0.005	6.65
Sm	0.019	n.d.	1.89	1.63	3.43	2.16	2.16	0.124	1.98	0.009	1.40
Eu	0.014	n.d.	0.596	0.093	0.419	0.058	0.052	0.064	0.074	0.002	0.809
Gd	0.028	n.d.	2.79	3.32	3.36	3.25	3.47	0.247	4.02	n.d.	2.33
Dy	0.029	0.007	3.65	3.84	4.81	4.33	4.94	0.395	4.47	0.032	3.14
Er	0.047	0.009	1.82	2.27	2.13	2.44	2.68	0.484	2.49	0.020	2.22
Yb	0.065	0.033	1.58	2.18	2.38	2.78	2.39	0.445	2.52	0.043	2.08
Lu	0.016	n.d.	0.268	0.300	0.392	0.463	0.432	0.085	0.427	0.010	0.341
Hf	0.001	0.002	1.68	0.185	2.88	0.221	0.265	0.022	0.272	0.002	0.267

Oliv.: olivine; Enst.: enstatite; Diop.: diopside, LCpx: Low-Ca clinopyroxene; Plag.: plagioclase; Neph.: Nepheline;
Melt Inc.: melt inclusion; Meso.: mesostasis; Alt.: an alterated part

Table 13: Major and trace element abundances in Ch69 determined by the SEM-EDX and the ion microprobe.

	Ch69-2-12 Alt.(Neph.)	Ch69-2-14 Diop.	Ch69-2-17 Enst.	Ch69-2-19 Enst.	Ch69-2-20 LCpx	Ch69-3-4 Diop.	Ch69-3-8 Neph.	Ch69-4-1 Plag.	Ch69-4-2 Diop.	Ch69-4-18 Oliv.	Ch69-6-8 LCpx	Ch69-6-9 Plag.	Ch69-6-18 Oliv.	Ch69-7-7 Enst.
(Wt. %)														
SiO_2	41.94	55.57	57.4	56.73	56.23	56.47	41.34	49.18	56.38	41.15	56.72	49.26	40.98	56.75
TiO_2	n.d.	0.50	0.06	0.15	0.23	0.54	n.d.	n.d.	0.35	n.d.	0.26	n.d.	0.05	0.06
Al_2O_3	33.69	3.56	1.5	1.52	2.38	2.29	34.84	33.33	2.56	0.51	2.65	33.27	0.76	1.26
Cr_2O_3	n.d.	0.51	0.38	0.53	0.85	0.46	n.d.	0	0.41	0.17	0.59	n.d.	0.14	0.41
MgO	0.31	24.63	39.2	38.50	36.29	24.71	n.d.	0.63	23.78	55.75	31.72	0.63	56.23	39.36
MnO	n.d.	n.d.	0.04	0.15	0.16	0.17	n.d.	n.d.	0.07	0.01	0.16	n.d.	0.02	0.03
FeO	0.16	0.38	0.56	0.46	0.67	0.4	0.01	0.41	0.41	1.37	0.48	0.54	0.28	0.43
CaO	2.36	14.85	0.43	0.59	2.38	14.96	1.49	13.85	16.04	0.15	7.14	13.59	0.35	0.36
NiO	n.d.	n.d.	n.d.	n.d.	n.d.	n.d.	0.04	n.d.	n.d.	0.05	n.d.	n.d.	n.d.	0.11
Na_2O	20.16	n.d.	0.34	0.67	0.49	n.d.	20.84	2.48	n.d.	0.55	0.24	2.55	0.75	0.61
K_2O	1.32	n.d.	0	0.04	n.d.	n.d.	1.45	n.d.	n.d.	n.d.	n.d.	n.d.	0.01	n.d.
P_2O_5	0.05	n.d.	0.05	0.37	0.16	n.d.	n.d.	0.12	n.d.	0.15	0.05	0.16	0.22	0.31
SO_3	n.d.	n.d.	0.06	0.25	0.16	n.d.	n.d.	n.d.	n.d.	0.14	n.d.	n.d.	0.21	0.3
Cl	n.d.	n.d.	n.d.	0.06	n.d.	n.d.	n.d.	n.d.	n.d.	n.d.	n.d.	n.d.	0.01	0.03
Total	100	100	100	100	100	100	100	100	100	100	100	100	100	100
($\mu g\ g^{-1}$)														
Sr	45.7	15.2	1.41	42.5	4.78	43.6	25.5	144	12.2	0.247	12.1	188	0.030	0.370
Y	5.02	18.7	1.41	4.77	26.5	84.4	7.73	0.552	60.0	0.222	5.61	0.543	0.311	0.226
Zr	31.0	16.4	2.46	10.5	50.9	169	7.97	0.346	143	0.278	6.20	2.72	0.123	0.342
Nb	2.05	0.038	0.032	0.056	0.214	0.331	0.997	0.058	0.216	0.002	0.024	0.152	0.001	0.006
Ba	2.89	3.96	7.78	71.2	30.6	42.6	3.02	5.06	5.06	0.465	3.52	3.17	n.d.	2.76
La	2.98	1.14	0.603	1.41	4.54	8.34	1.01	0.157	4.27	0.019	0.492	0.289	n.d.	0.238
Ce	6.31	2.90	1.26	2.54	10.3	23.2	2.15	0.443	13.0	0.023	1.39	0.541	n.d.	0.294
Pr	0.639	0.515	0.167	0.282	1.43	3.62	0.260	0.038	2.14	0.004	0.175	0.102	n.d.	0.025
Nd	2.63	2.77	0.492	1.34	7.57	20.6	1.59	0.301	11.9	0.014	1.23	0.325	n.d.	0.150
Sm	0.851	1.17	0.120	0.424	1.71	6.98	0.593	0.037	4.18	0.005	0.173	0.028	0.005	0.022
Eu	0.342	0.120	0.116	0.289	0.071	0.703	0.199	0.585	0.331	n.d.	0.685	0.738	n.d.	0.066
Gd	0.322	1.95	0.189	0.880	4.71	10.2	1.08	0.030	7.51	0.020	0.405	0.069	n.d.	0.048
Dy	0.536	2.90	0.173	0.626	3.97	12.1	1.21	0.151	8.36	0.025	0.635	0.064	0.016	0.041
Er	0.254	1.53	0.206	0.533	2.34	8.00	0.584	0.053	4.90	0.052	0.733	0.106	0.049	0.061
Yb	0.329	1.82	0.223	0.409	2.62	7.09	0.719	0.027	4.81	0.046	0.761	0.040	0.070	0.049
Lu	0.121	0.300	0.031	0.083	0.376	1.23	0.090	0.004	0.755	0.004	0.094	0.008	0.022	0.007
Hf	0.448	0.191	0.009	0.064	0.237	0.988	0.515	0.031	0.527	0.000	0.055	0.015	0.001	0.001

Table 14: Major and trace element abundances in Ch145 determined by the SEM-EDX and the ion microprobe.

	Ch145-1-2 Diop.	Ch145-1-3 Diop.	Ch145-1-4 Pig.	Ch145-1-10 Plag.	Ch145-1-12 LCpx	Ch145-1-13 Oliv.	Ch145-2-1 Diop.	Ch145-4-2 Meso.	Ch145-5-2 Enst.
(Wt. %)									
SiO_2	53.11	54.61	56.98	45.35	55.64	41.25	55.09	48.82	57.85
TiO_2	0.72	0.74	0.30	0.01	0.41	n.d.	0.67	0.01	0.16
Al_2O_3	5.46	3.30	2.33	34.59	2.88	0.24	2.66	27.32	0.93
Cr_2O_3	0.80	0.53	0.70	0.09	0.75	0.03	0.38	0.22	0.46
MgO	23.64	23.70	35.15	0.62	34.01	55.68	22.72	7.90	39.24
MnO	0.24	0.12	0.11	0.02	0.21	0.16	0.07	0.08	0.07
FeO	0.34	0.16	0.50	0.63	0.55	2.00	0.14	1.05	0.27
CaO	14.89	16.46	3.69	17.17	4.46	0.18	17.7	12.99	0.50
NiO	0.11	n.d.	n.d.	0.05	0.10	0.03	n.d.	0.08	0.02
Na_2O	0.26	0.20	0.20	1.16	0.48	0.39	0.27	1.14	0.22
K_2O	0.02	n.d.	n.d.	0.04	0.02	n.d.	0.01	0.03	0.03
P_2O_5	0.21	0.06	0.04	0.19	0.25	0.02	0.23	0.13	0.06
SO_3	0.20	0.12	n.d.	0.06	0.20	0.02	0.02	0.20	0.19
Cl	n.d.	n.d.	n.d.	0.01	0.04	0.01	0.04	0.02	n.d.
Total	100	100	100	100	100	100	100	100	100
($\mu g\ g^{-1}$)									
Sr	4.86	8.62	13.8	102	3.18	0.151	55.3	6.52	4.43
Y	9.58	17.5	6.77	3.56	4.57	0.488	10.6	4.37	1.09
Zr	14.9	31.2	11.8	10.7	9.53	0.352	17.7	10.6	3.77
Nb	0.053	0.086	0.030	1.73	0.037	0.002	0.067	1.01	0.012
Ba	11.9	6.47	10.4	16.0	14.61	0.086	10.8	2.39	16.3
La	1.43	2.05	0.896	1.94	1.26	0.002	1.08	0.547	0.243
Ce	4.56	5.05	2.26	5.39	3.04	0.018	3.26	1.36	0.661
Pr	0.703	0.792	0.292	0.696	0.344	0.002	0.533	0.151	0.0820
Nd	3.47	4.56	1.41	3.04	1.81	0.035	3.74	1.21	0.467
Sm	0.986	1.50	0.561	0.578	0.382	0.009	0.949	0.331	0.224
Eu	0.098	0.111	0.268	1.10	0.050	0.005	0.193	0.191	0.104
Gd	2.06	2.01	1.05	0.974	0.775	0.006	1.42	0.502	0.364
Dy	2.13	2.82	1.22	0.748	0.847	0.052	1.88	0.781	0.300
Er	1.15	1.63	0.807	0.484	0.551	0.030	1.05	0.453	0.194
Yb	1.05	1.81	0.940	0.349	0.706	0.128	1.16	0.584	0.237
Lu	0.187	0.339	0.131	0.109	0.096	0.008	0.129	0.056	0.027
Hf	0.080	0.137	0.077	0.264	0.066	0.004	0.123	0.195	0.021

Table 15: Major and trace element abundances in Ch159 determined by the SEM-EDX and the ion microprobe.

	CH159-5-3	Ch159-5-11	CH159-7-1	CH159-7-7	CH159-8-1	Ch159-8-4	Ch159-8-15	Ch159-8-20
	Enst.	Alt.	Neph.	LCpx	Meso.	Plag.	Plag.	Oliv.
(Wt. %)								
SiO_2	57.91	38.74	41.45	55.97	46.59	45.98	46.32	40.95
TiO_2	0.09	0.03	0.01	0.73	0.01	n.d.	0.05	0.02
Al_2O_3	1.01	1.54	34.36	2.50	33.49	33.93	33.78	0.17
Cr_2O_3	0.49	0.17	0.09	0.77	n.d.	0.04	0.02	0.02
MgO	39.07	32.97	0.16	34.49	0.53	0.57	0.55	52.7
MnO	0.07	0.14	n.d.	0.16	0.07	n.d.	n.d.	0.05
FeO	0.52	25.76	0.42	0.64	0.91	0.73	0.7	5.42
CaO	0.44	0.29	1.94	4.39	15.28	16.86	16.77	0.18
NiO	n.d.	0.22	0.06	0.08	0.05	0.17	n.d.	n.d.
Na_2O	0.25	0.14	19.4	0.11	2.28	1.56	1.54	0.38
K_2O	n.d.	n.d.	1.86	n.d.	0.04	0.02	0.01	n.d.
P_2O_5	n.d.	n.d.	0.17	0.03	0.26	0.08	0.20	n.d.
SO_3	0.15	n.d.	0.09	0.13	0.12	0.06	0.06	0.10
Cl	n.d.	n.d.	n.d.	n.d.	0.38	n.d.	n.d.	0.01
Total	100	100	100	100	100	100	100	100
($\mu g\ g^{-1}$)								
Sr	2.31	0.650	32.8	6.95	511	419	375	0.254
Y	0.503	0.334	3.18	8.04	0.526	0.245	0.257	0.181
Zr	1.21	0.856	4.66	8.89	0.106	0.133	0.168	0.104
Nb	0.008	0.003	0.496	0.015	0.013	n.d.	0.048	0.001
Ba	2.11	3.30	1.92	17.6	5.61	2.61	3.96	0.354
La	0.267	0.079	0.902	0.376	0.217	0.141	0.170	0.043
Ce	0.466	0.151	1.27	0.935	0.418	0.186	0.319	0.075
Pr	0.109	0.013	0.441	0.132	0.077	0.022	0.123	0.014
Nd	0.571	0.061	1.37	0.944	0.273	0.173	0.219	0.089
Sm	0.067	0.029	0.281	0.256	0.302	0.047	0.138	0.023
Eu	0.209	0.015	0.275	0.220	0.555	0.460	0.208	0.063
Gd	0.557	0.010	0.362	0.772	0.031	0.040	n.d.	0.019
Dy	0.077	0.053	0.481	1.11	0.050	0.021	0.009	0.053
Er	0.174	0.043	0.355	0.712	0.156	0.118	0.070	0.034
Yb	0.292	0.042	0.557	0.735	0.199	0.052	0.012	0.062
Lu	0.094	0.009	0.068	0.152	0.004	n.d.	0.009	0.013
Hf	0.013	0.007	0.284	0.065	0.038	n.d.	n.d.	n.d.

Table 16: Major and trace element abundances in Ch162 determined by the SEM-EDX and the ion microprobe.

	CH162-2-1 Melt Inc.	CH162-2-5,6 Melt Inc.	CH162-2-14 Meso.	CH162-4-1 Oliv.	CH162-4-5,7 Meso.	CH162-5-10 Oliv.	CH162-7-4 Diop.	CH162-8-1 Meso.
(Wt. %)								
SiO_2	47.46	34.28	47.39	41.39	44.94	40.97	53.39	46.76
TiO_2	0.75	0.73	n.d.	0.08	n.d.	0.08	1.32	0.02
Al_2O_3	27.63	21.57	32.5	0.27	27.24	0.36	4.61	32.56
Cr_2O_3	0.19	0.28	n.d.	0.12	0.02	0.20	0.62	0.03
MgO	4.70	11.81	0.70	56.14	8.53	56.75	21.2	1.08
MnO	n.d.	n.d.	n.d.	0.04	n.d.	0.04	0.02	n.d.
FeO	0.24	9.96	1.40	1.26	4.46	0.62	0.33	1.04
CaO	17.2	15.35	15.92	0.32	12.65	0.32	17.95	16.08
NiO	n.d.	0.45	0.01	n.d.	0.02	0.10	0.09	0.01
Na_2O	1.64	0.36	2.02	0.31	1.88	0.36	0.18	2.07
K_2O	n.d.	0.02	n.d.	n.d.	0.02	0.05	n.d.	0.02
P_2O_5	0.18	0.09	0.05	0.04	0.07	n.d.	0.14	0.21
SO_3	0.01	5.07	n.d.	0.04	0.12	0.11	0.08	0.08
Cl	n.d.	0.03	n.d.	n.d.	0.04	0.04	0.04	0.03
Total	100	100	100	100	100	100	100	100
($\mu g\ g^{-1}$)								
Sr	102	99.7	145	1.62	176	1.95	9.92	120
Y	25.3	29.4	5.85	0.447	9.69	0.252	18.9	1.23
Zr	71.9	75.3	13.2	0.441	31.7	0.085	20.0	2.27
Nb	0.172	5.11	0.935	0.005	2.59	0.001	0.029	0.679
Ba	49.4	26.8	6.24	2.30	11.5	0.595	4.82	8.76
La	3.87	4.44	0.924	0.221	1.67	0.029	0.841	0.898
Ce	9.46	10.6	2.21	0.167	3.81	0.050	2.51	1.73
Pr	1.42	1.73	0.317	0.061	0.751	0.003	0.711	0.669
Nd	7.66	10.6	1.85	0.450	4.37	0.009	4.45	3.57
Sm	2.20	5.61	0.417	0.558	1.76	0.005	3.64	3.32
Eu	0.670	1.06	0.735	0.136	0.846	0.011	0.788	1.60
Gd	2.92	4.08	0.709	0.641	1.76	0.010	3.40	2.67
Dy	4.62	5.73	0.661	0.127	2.49	0.019	4.18	2.45
Er	2.72	3.52	0.302	0.252	0.931	0.045	2.97	2.21
Yb	2.90	2.59	0.696	0.164	1.02	0.039	2.76	1.73
Lu	0.372	0.725	0.038	0.034	0.299	0.018	0.752	0.375
Hf	0.241	4.29	0.281	0.091	1.65	n.d.	0.329	3.85

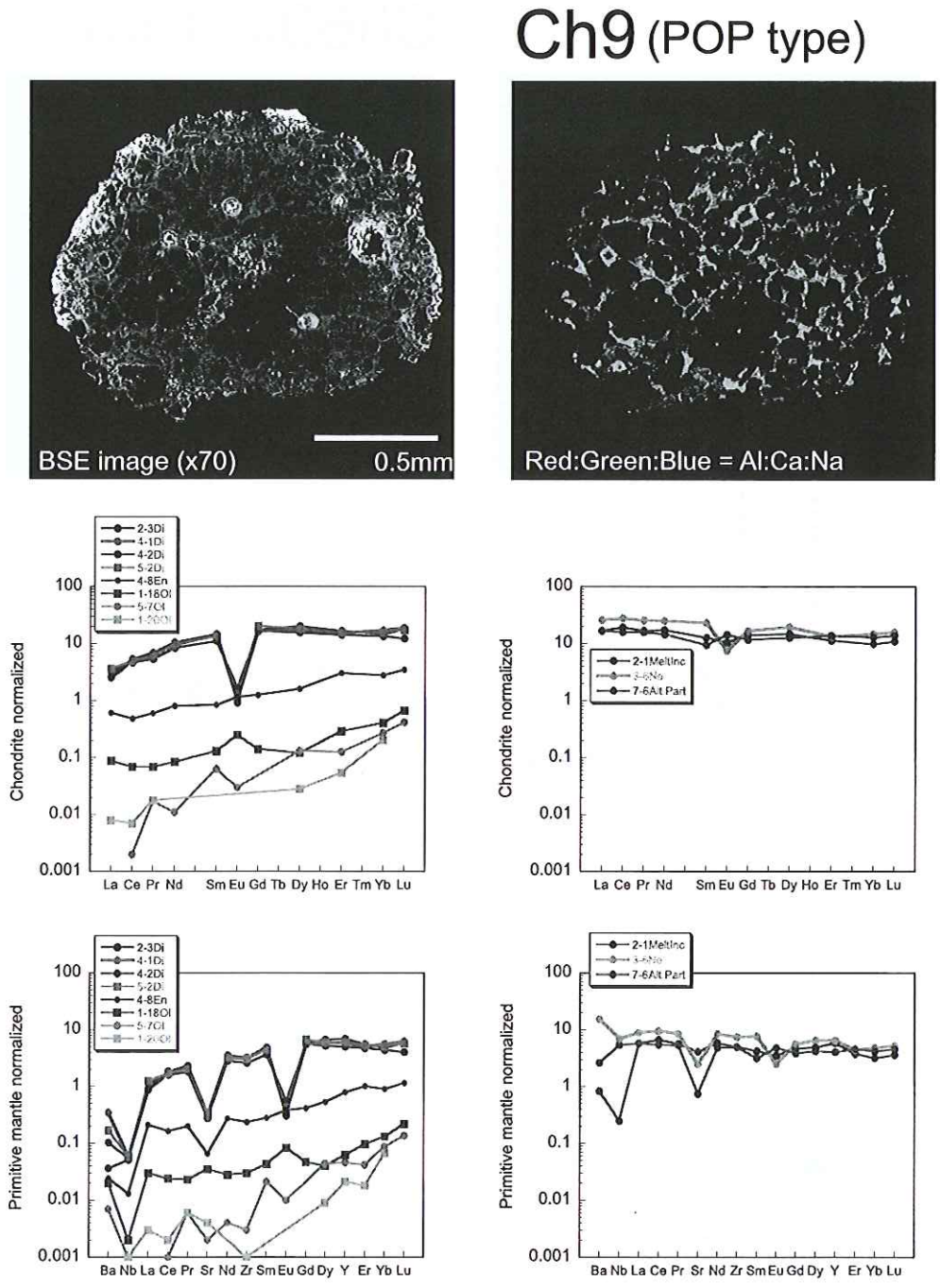

Fig. 15: REE and trace element patterns for components of Allende chondrule, Ch9, BSE and compositional mapping images. Abbreviations are as follows; Di: diopside, En: enstatite, Ol: olivine, LCpx: Low-Ca clinopyroxene, Pl: plagioclase, Meso: mesostasis, Melt Inc: melt inclusion, Ne: nepheline, Alt. Part: altered part.

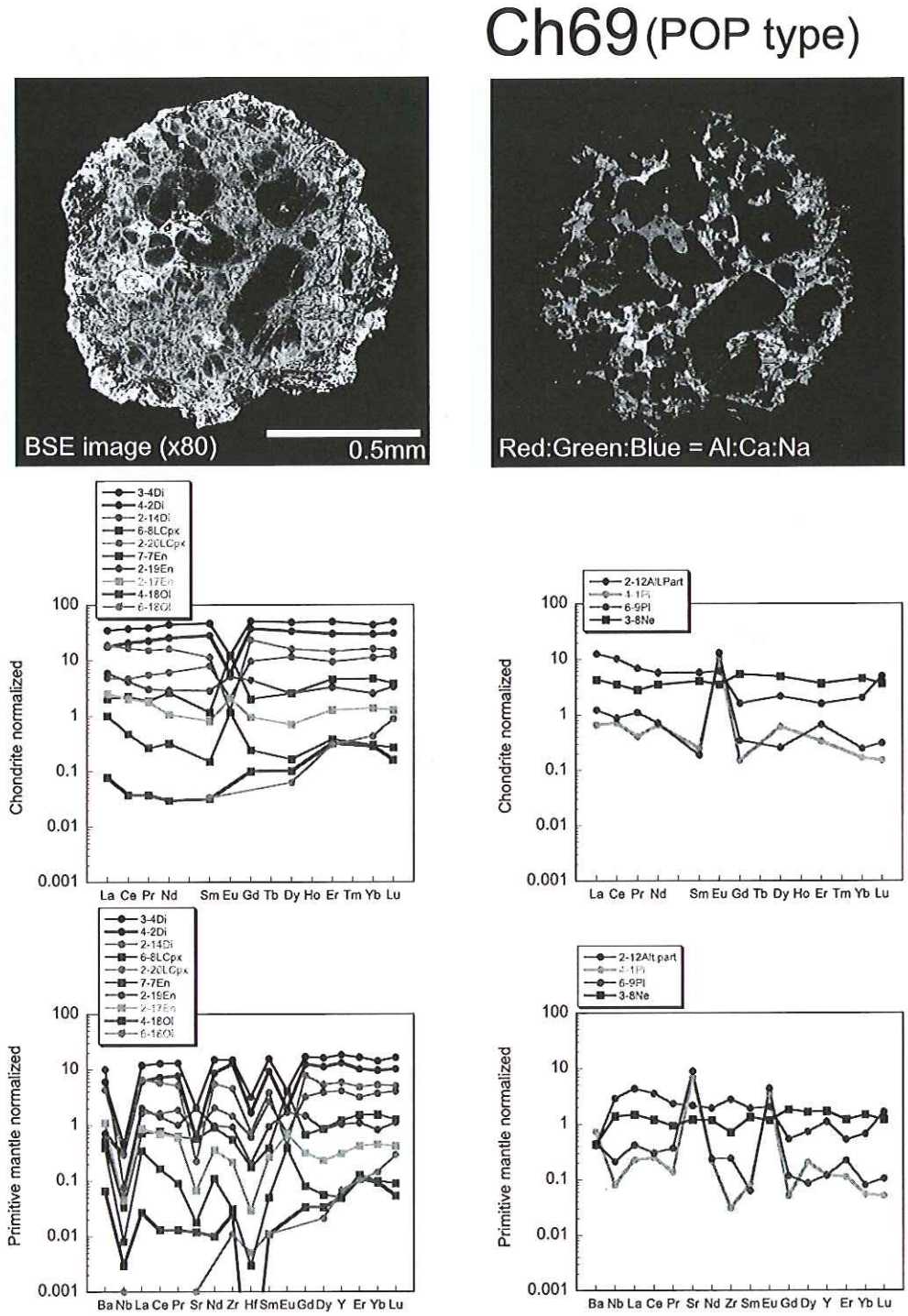

Fig. 16: REE and trace element patterns for components of Allende chondrule, Ch69, BSE and compositional mapping images. See Fig. 15 caption for abbreviations.

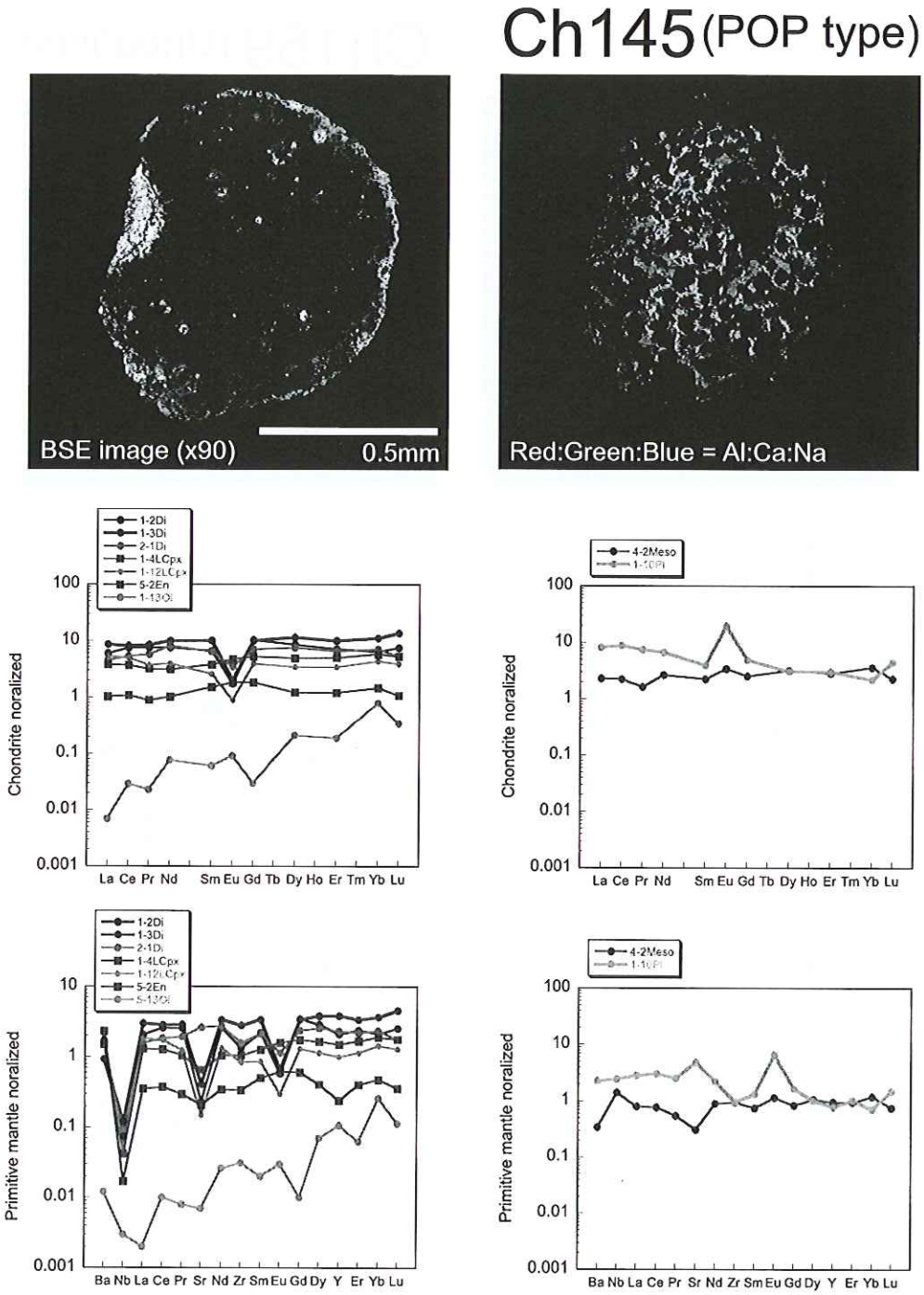

Fig. 17: REE and trace element patterns for components of Allende chondrule, Ch145, BSE and compositional mapping images. See Fig. 15 caption for abbreviations.

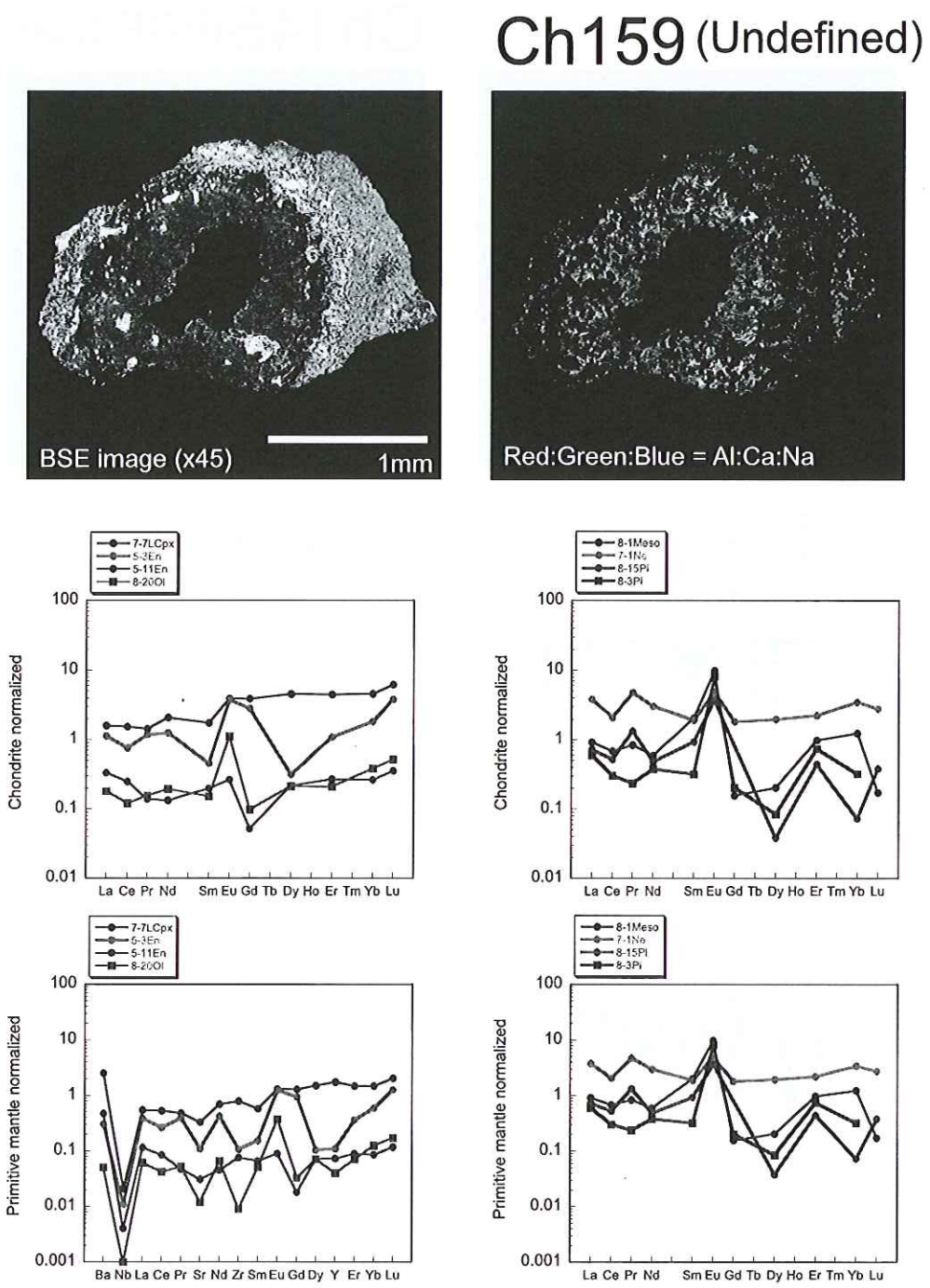

Fig. 18: REE and trace element patterns for components of Allende chondrule, Ch159, BSE and compositional mapping images. See Fig. 15 caption for abbreviations.

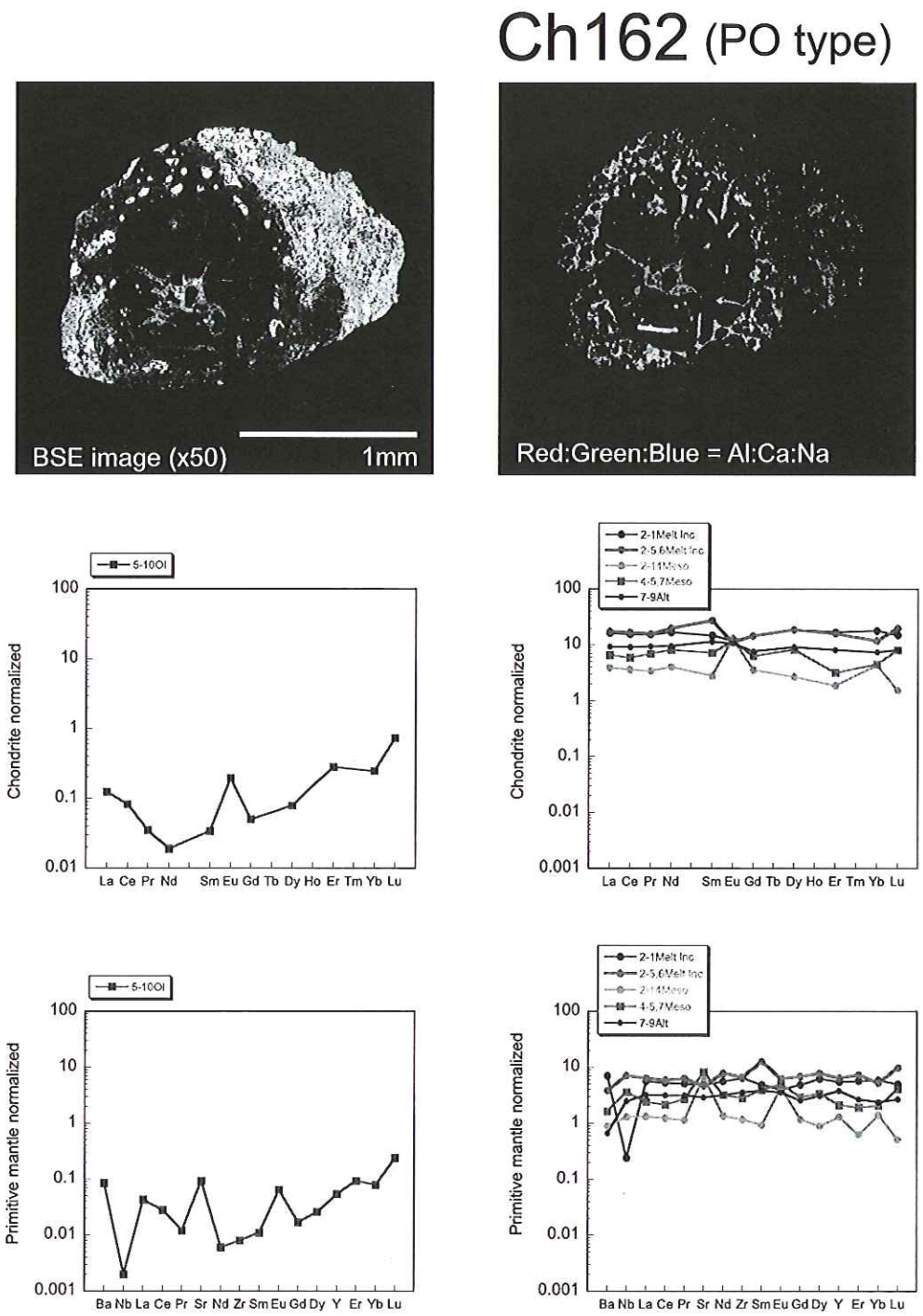

Fig. 19: REE and trace element patterns for components of Allende chondrule, Ch162, BSE and compositional mapping images. See Fig. 15 caption for abbreviations.

Table 17: Element abundances (μg g^{-1}) in chondrules determined by the ICP-MS.

sample	Ch9	blank	Ch69	blank	Ch145	blank	Ch159	blank	Ch162	blank
weight* (mg)	0.468	corr(%)	0.426	corr(%)	0.148	corr(%)	0.609	corr(%)	0.0248	corr(%)
Li	0.890	2	1.613	1	1.72	3	1.73	1	1.04	23
B										
Y	5.92	0	5.87	0	4.58	0	8.50	0	3.84	0
Zr										
Nb										
Cs	0.0435	2	0.0323	4	0.0157	19	0.0372	2	0.00644	78
Ba	4.34	0.3	3.77	0.4	6.97	1	6.08	0.1	5.25	5
La	0.623	0.5	0.619	1	0.485	2	0.913	0.3	0.273	20
Ce	1.96	0.1	1.79	0.1	1.59	0.3	2.55	0.04	0.931	3
Pr	0.290	0.2	0.296	0.2	0.263	1	0.417	0.1	0.159	7
Eu	0.131	2	0.165	2	0.163	5	0.218	1	0.0491	52
Gd	0.723	0.7	0.719	1	0.485	4	1.05	0.4	0.221	36
Tb	0.140	0.6	0.140	1	0.106	3	0.204	0.3	0.0597	23
Dy	0.985	0.4	1.01	0.5	0.763	2	1.42	0.2	0.423	16
Ho	0.209	0.4	0.217	1	0.157	2	0.309	0.2	0.0726	23
Er	0.593	0.4	0.592	1	0.421	2	0.872	0.2	0.277	17
Tm	0.103	0.9	0.0975	1	0.0800	4	0.143	1	0.0315	40
Yb	0.566	0.6	0.608	1	0.550	2	0.858	0.3	0.288	22
Lu	0.095	1	0.0918	2	0.0708	5	0.139	1	0.0413	37
Hf										
Ta										
Pb	0.48	4.2	0.31	8	0.47	15	0.74	2.2	3.77	11
Pb	0.482	4	0.311	8	0.465	15	0.740	2	3.77	11
Th	0.108	2	0.0946	3	0.0705	12	0.164	1	0.00481	92
U	0.0293	4	0.0243	6	0.0161	22	0.0272	3	-	
weight (mg)	0.544		0.696		0.155		2.15		1.83	
B	0.394	51	0.0720	82	0.656	69	0.122	46	0.299	29
Zr	12.8	9	12.7	8	9.28	34	16.6	2	7.34	5
Nb	0.858	0.4	1.11	0.3	0.504	3	0.697	0.1	0.546	0.2
Hf	0.220	8	0.233	6	0.299	18	0.425	1	0.176	3
Ta	0.0491	64	0.0320	68	0.147	67	0.0125	64	0.0149	63

* These samples were weighed as solutions.

Table 18: Rb, Sr, Sm and Nd isotope compositions of Allende chondrules.

sample	weight* (mg)	Rb (μg g^{-1})	blank corr (%)	Sr (μg g^{-1})	blank corr (%)	Rb (ng)	Sr (ng)	^{87}Rb/^{86}Sr	$2\sigma_{mean}$	^{87}Sr/^{86}Sr	2σ mean
Ch9	0.667	1.35	0.04	9.89	0.18	0.90	6.6	0.395	0.0005	0.724171	± 24
Ch69	0.418	0.527	0.2	16.3	0.14	0.22	6.8	0.0937	0.0002	0.704724	± 22
Ch145	0.155	0.558	0.4	26.6	0.25	0.087	4.1	0.0607	0.0001	0.702784	± 23
Ch159	0.848	1.30	0.04	29.9	0.05	1.1	25	0.125	0.0002	0.707166	± 13
Ch162	0.0248	0.387	4	12.4	3.21	0.010	0.31	0.0901	0.0002	0.704774	± 50

sample	Sm (μg g^{-1})	blank corr (%)	Nd (μg g^{-1})	blank corr (%)	Sm (ng)	Nd (ng)	^{147}Sm/^{144}Nd	$2\sigma_{mean}$	^{143}Nd/^{144}Nd	$2\sigma_{mean}$
Ch9	0.580	0.06	1.63	0.09	0.39	1.1	0.215	0.0003	0.513013	± 19
Ch69	0.541	0.09	1.59	0.13	0.23	0.66	0.206	0.0003	0.512927	± 49
Ch145	0.426	0.3	1.21	0.48	0.066	0.19	0.214	0.0004	0.513837	± 195
Ch159	0.775	0.04	2.25	0.05	0.66	1.9	0.208	0.0003	0.513257	± 60
Ch162	0.265	3	0.756	4.62	0.007	0.019	0.215	0.0008	0.511300	± 986

* These samples were weighed as solutions.

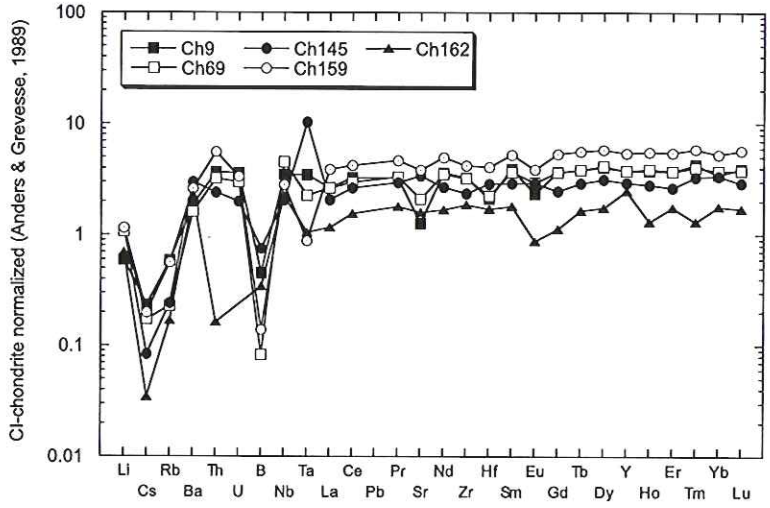

Fig. 20: CI-chondrite normalized element abundances of chondules.

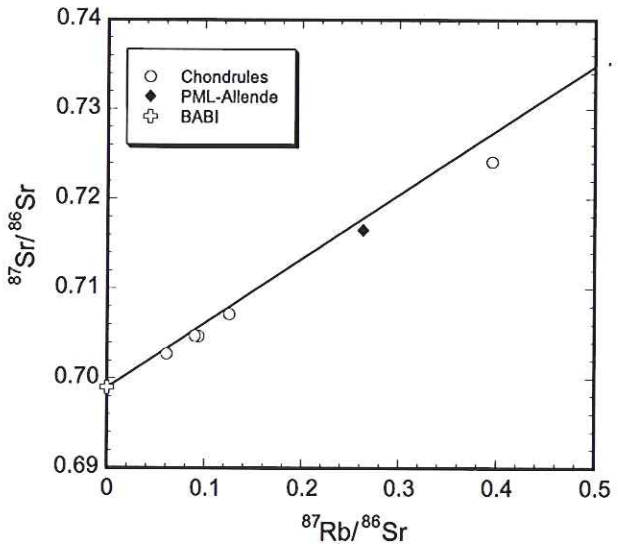

Fig. 21: Rb-Sr diagram for chondrules. BABI (basaltic achondrite best initial, $^{87}Sr/^{86}Sr$ = 0.69899 ± 0.000047) is from Papanastassiou & Wasserburg (1969). Analitical error falls within the symbols.

along with concentrations of these elements, are given in Table 18. The sample weights of the chondrules for these isotope analyses were extraordinary small, 0.025 to 0.85 mg, and the amounts of Sr and Nd loaded onto the filaments for the mass spectrometry ranged from 0.3 to 25 ng and 0.02 to 2 ng, respectively. These loaded amounts are one to three orders of magnitudes smaller than those in standard isotope analyses of these elements by TIMS. However, the analytical errors for the chondrules, except for Ch162, are comparable to those for terrestrial samples with large amounts of sample loaded; for example, 1 μg and 0.5 μg for

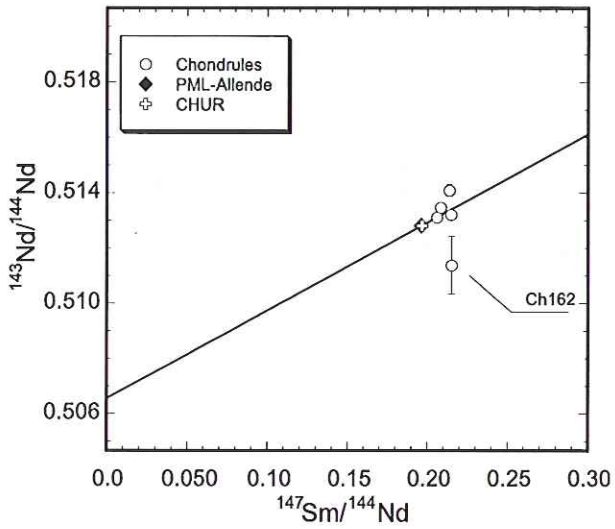

Fig. 22: Sm-Nd diagram for chondrules. CHUR (chondritic uniform reservoir, $^{147}Sm/^{144}Nd = 0.1967$ and $^{143}Nm/^{144}Nd = 0.512638$) is from DePaolo & Wasserburg (1976).

Sr and Nd isotope analyses, respectively. Even in the trace sample analyses, blank levels were extremely small (less than 0.3 and 0.5 % for Sr and Nd, respectively) except for in the analyses of Ch162, resulting for the most part in negligible blank corrections. Thus, blank corrections were carried out only for the isotope results for sample Ch162. The Sr isotopic compositions of the individual chondrules are plotted against Rb/Sr ratios in Fig. 21. All data plot below the 4.55 Ga model isochron line and form an apparent isochron with an age of 4.359 ± 0.140 Ga (Initial $^{87}Sr/^{86}Sr = 0.69895 \pm 0.00041$, MSWD = 249). On the other hand, the data for chondrules are plot fairly tightly and near CHUR and the bulk PML-Allende powder on the 4.56 model isochron (except for the sample Ch162; see Fig. 22). This is consistent with the observation that the REE patterns of these chondrules obtained by ICP-MS (Fig. 20) are flat and that their Sm/Nd ratios are nearly constant as chondritic. These observations indicate that isotope analyses for Rb-Sr and Sm-Nd systems, together with trace element analyses by ICP-MS using extremely small amounts of sample (<1 mg of chondrules) are practical in studies evaluating the evolution of extraterrestrial materials and employing the methods established in the CASTEM at PML.

5. EVALUATION OF ANALYTICAL PERFORMANCE, SUGGESTION AND PERSPECTIVE

5.1 Evaluation

In April 2000, we officially proposed to participate in determining element abundances and isotope compositions, along with textural analyses, of the samples provided from ISAS for this analytical contest as follows:

(1) 53 elements for quantitative analyses using Q-type and sector-type ICP-MSs with calibration and isotope dilution methods.

(2) Li, B, Sr, Ce, Nd, Os and Pb isotope analyses of the samples by TIMSs, provided that

the amounts of the elements are large enough for the TIMS analyses (particularly a factor for the Li, B and Ce analyses).

(3) Ion microprobe analyses for more than 30 elements in minerals with a spot size around 10 μm using a Cameca ims-5f, and Li, B and O isotope analyses using a highly sensitive ion microprobe, a Cameca ims-1270 if the analytical techniques are available during the period of the contest.

(4) Description of mineral phases and textures in the fragment samples by EPMA and SEM-EDX.

(5) Determination of bulk major element compositions of the samples by X-ray fluorescence (XRF) methods.

Analytical performance on the above items, which we achieved in the period of this competition (over 3 months), may be evaluated as follows:

To (1): 55 elements were determined with analytical errors less than 10% (1σ) using approximately 30 mg each of the samples 1C and 2C provided by ISAS. This proposed work, on the quantitative elemental analyses using ICP-MS, has clearly been accomplished. Because fragment samples were not provided by ISAS, we attempted to determine the bulk trace element concentrations, together with Sr and Nd isotopic compositions, in individual chondrules. Consequently, concentrations for 24 trace elements were obtained for extremely small samples (<0.609 mg). If necessary, another at least 15 elements could be determined for these small samples using ICP-MS techniques established at PML.

To (2): We successively separated B, Pb, Li, Rb, Sr, Sm and Nd from approximately 70 mg of each of the samples for TIMS analyses. In addition, Sr, Nd and Re and Os were separated from aliquots of the sample solutions used for trace element analyses by ICP-MS. However, the Ce isotope analyses were not undertaken for the competition samples, because the abundances of Ce (50 ng and 90 ng) in 70 mg samples (1C and 2C, respectively) determined by ICP-MS are too low to allow precise measurement of their Ce isotopic composition by TIMS. Presently, more than 250 ng of Ce are required for precise isotope measurements in our laboratory. The Ce isotope work could be possible if larger amounts of sample become available.

Prior to the preparation of the samples for these multi-isotope analyses, the concentrations of these elements were obtained from small aliquots of the sample solutions used for trace element analyses with ICP-MS. This resulted in our knowing the abundances of these elements in the samples prior to the isotope work and made it possible for us to carry out simulation isotope analyses using amounts of the elements similar to those in the unknown samples. This improved the reliability of the isotope analyses for the extremely small amounts of precious sample. Therefore, we believe that our performance on the multi-isotope analyses for both the competition samples and the chondrules satisfactorily demonstrates our ability to do the isotopic work we proposed on appropriate materials.

To (3): Probe analyses of minerals and glasses in the chondrules were performed on 30 elements by a combination of ion microprobe (Cameca ims 5f) and EDX-SEM work. In this contest, only powdered samples were provided, and we had expected to receive fragment samples in addition to the powdered sample. Therefore, we undertook only basic probe analyses using these instruments, which have been routinely employed at PML in other studies of terrestrial and extraterrestrial samples. We measured only 16 trace elements in the constituent minerals and glasses in chondrules using the ion microprobe. However, it is possible to increase the

number of elements for ion probe analyses to as many as those determined by ICP-MS and TIMS, if necessary. We are able to make accurate standard materials for trace element and isotope measurements by ion microprobe by careful characterization with ICP-MS and TIMS of materials which have matrices similar to those of the samples to be measured by SIMS. We have been assembling standard materials by analyzing homogeneous natural minerals and glasses, and by preparing synthesized glasses doped with specific elements and isotopes using excellent facilities for high pressure and temperature experiments at the ISEI (particularly the piston cylinders).

All isotope measurements we proposed were not carried out for the chondrule samples. The installation of the Cameca ims-1270 ion microprobe at PML was completed in April 2000, and we have first focused on developing U-Pb zircon dating with this instrument. We established our methods to date small regions of zircons (as small as several μm in diameter) by the end of November 2000 (Kobayashi *et. al.*, 2000). We have also been involved in the preparation of zircon standards for ion probe analysis using conventional TIMS techniques for the precise determination of Pb, U and Th isotopes in the zircons. Boron isotope analysis using the -5f ion microprobe was already developed for B-rich minerals such as tourmaline using our own standards measured by TIMS (Nakano & Nakamura, 2001). However, these ion microprobe techniques could not be applied to the chondrules because of the extremely low concentrations of these elements in mineral phases in the chondrules. We are now preparing Li, B and Pb isotope standard materials, for use on the ims-1270, that will soon make it possible for us to determine isotopic compositions for glass inclusions and, especially, Li and B isotope compositions in olivine and mesostasis in chondrules.

To (4): The textural and compositional analyses were successfully undertaken for the center portions of chondrules by cutting them with a dicing saw into three pieces. These analyses were combined with trace element analyses obtained by ion microprobe.

To (5): XRF analyses were not undertaken for the competition samples because sample amounts were insufficient to make glass bead samples for major element analyses.

5.2 Suggestion

Based on the B contents and isotopic compositions, we conclude that the powdered samples were extensively contaminated by B from the glass vials, which are made of borosilicate with ~4 wt% of B. Therefore, the use of such a glass vial must be prohibited for the preservation of samples collected on this mission. We suggest that the material of the containers for both the preservation and curation of samples must be same as that of the sample capsule on the MUSES-C spacecraft. This will minimize the contamination to the samples from materials on Earth.

5.3 Perspective

In the CASTEM at PML, quantitative analyses of Se, Ag, Cd, In, Te, Hg, Tl and Bi will soon be available, in addition to the analyses of the other 55 elements using the ICP-MSs. Furthermore, we will be able to carry out precise Li, B, O, Mg, Cr, Ni and Fe isotope analyses using the Cameca ims-1270 within the next 1 to 3 years. It will be possible for other parties with other expertise to jointly own the polished thin sections obtained by cutting the small samples into three pieces and used for the probe analyses and petrographic investigations in this study. This will provide for the most comprehensive investigation possible on the extremely small and precious samples directly returned from the asteroid by the MUSES-C mission. Based on our

analytical experience, all of the analyses carried out in this competition (or a similar volume of work on other similar materials) could be completed within 50 days, if we could concentrate on only this specific geochemical project during that 50-day period.

ACKNOWLEDGEMENTS

Many people were involved in setting up the CASTEM since 1987. We appreciate former post-doctoral fellows and graduate students, Yoshiyuki KOIDE, Tsuyoshi ISHIKAWA, Tomoyuki SHIBATA, Masako YOSHIKAWA, Yoshiyuki IIZUKA, Toshio NAKANO, Reiko SADACHIKA and Mayumi NAKANISHI for their contributions to developing analytical techniques and building the clean rooms at PML. Our thanks are also extended to the former directors of ISEI, Profs. Shun-ichi AKIMOTO, Yoshito MATSUI and Ikuo KUSHIRO for their support and encouragement to build a geochemistry laboratory at Misasa. We thank former president of Okayama University, Prof. Futami KOSAKA and the former chief of an accounting section of ISEI, Mr. Jun-ichi ICHIMURA, for their financial support and encouragement. Without the full support of these people, it would have been extremely difficult to establish the CASTEM, and to participate in this analytical competition to demonstrate our analytical capabilities using the many modern analytical facilities and fine techniques we have developed. We also express our gratitude to Dr. Gray BEBOUT for his efforts to improve this report. Finally, we thank our colleagues in PML, Sophie ALVES, Tomohiro USUI, Takeru MORIYAMA, Estelle ROSE, Nobutaka AKIYOSHI, Nobuko TAKEUCHI and Manami TANAKA, for their assistance.

REFERENCES

Anders, E. & N. Grevesse, Abundances of the elements: Meteoritic and solar, *Geochim. Cosmochim. Acta*, **53**, 197–214, 1989.

Birck, J.L., M. Roy Barman & F. Capmas, Re-Os isotopic measurements at the femtomole level in natural samples, *Gestand. Newslett.*, **20**, 19–27, 1997.

DePaolo, D. J. & G. J. Wasserburg, Nd isotopic variations and petrogenetic models, *Geophys, Res. Letters*, **3**. 249–252, 1976.

Gerstenberger, H., & Haase, G., A highly effective emitter substance for mass spectrometric Pb isotope ratio determinations, *Chem. Geol.*, **136**, 309–312, 1997.

Imai, N., S. Terashima, S. Itoh, & A. Ando, 1994 compilation values for GSJ reference samples, "Igneous rock series", *Geochem. J.*, **29**, 91–95, 1995.

Ishikawa, T. & E. Nakamura, Suppression of B volatilization from a hydrofluoric acid solution using a B-mannitol complex, *Anal. Chem.*, **62**, 2612–2616, 1990.

Jarosewich, E., R. S. Clarke, Jr. & J. N. Barrors, The Allende Meteorite Reference Sample, Smithon. *Contrib. Earth Sci.*, **27**, 1–12, 1987.

Koide, Y., & E. Nakamura, Pb isotope analyses of standard rock samples, *Mass spectrosc.*, **38**, 241–252, 1990.

Kobayashi, K., Usui, T. & E. Nakamura, Zircon age dating by dynamic multi-collection method using high resolution secondary ion mass spectrometer, *Abstract for 1999 Annu. Meeting of the Japan Assoc. Min. Petro. Econ. Geol. at Tokushima,*, **38**, 2000.

Kuritani, T. & E. Nakamura, Precise isotope analysis of nanogram-level Pb for natural rock samples without use of double spikes, *Chem. Geol.* **186**, 31–43, 2002.

Lindner, M., R.J. Leich, G.P. Russ, J.M. Basan, & R.J. Borg, Direct determination of the half-life of ^{187}Re, *Geochim. Cosmochim. Acta*, **53**, 1597–1606, 1989.

Makishima, A. & E. Nakamura, Precise measurement of cerium isotope composition in rock samples, *Chem. Geol. (Isotope Geosci.)*, **94**, 1–11, 1991a.

Makishima, A. & E. Nakamura, Calibration of Faraday cup efficiency in a multicollector mass spectrometer, *Chem. Geol. (Isotope Geosci.)*, **94**, 105–110, 1991b.

Makishima, A., E. Nakamura & S. Akimoto, Investigation of the Bias in a Secondary Electron Multiplier of Finigan-MAT 261 Mass spectrometer for the Quantitative Analysis of Rare-Earth Elements in Rock Samples, *Tech. Report of ISEI, Okayama Univ., Ser. B*, **10**, 1–19, 1991.

Makishima, A., E. Nakamura, & T. Nakano, Determination of B in silicate samples by direct aspiration of sample HF solutions into ICPMS, *Anal. Chem.*, **69**, 3754–3759, 1997a.

Makishima, A., & E. Nakamura, Suppression of matrix effects in ICP-MS by high power operation of ICP: Application to precise determination of Rb, Sr, Y, Cs, Ba, REE, Pb, Th and U at ng g^{-1} levels in milligram silicate samples, *Geostand. Newslett.*, **21**, 307–319, 1997b.

Makishima, A., E. Nakamura, & T. Nakano, Determination of zirconium, niobium, hafnium and tantalum at ng g^{-1} levels in geological materials by direct nebulisation of sample HF solution into FI-ICP-MS, *Geostand. Newslett.*, **23**, 7–20, 1999.

Makishima, A. & E. Nakamura, Determination of molybdenum, antimony and tungsten at sub μg g^{-1} levels in geological materials by ID-FI-ICP-MS, *Geostand. Newslett.*, **23**, 137–148, 1999.

Makishima, A., & E. Nakamura, Determination of titanium at μg g^{-1} levels in milligram amounts of silicate materials by isotope dilution high resolution inductively couples plasma mass spectrometry with flow injection, *J. Anal. At. Spectrom.*, **15**, 263–267, 2000.

Makishima, A. & E., Nakamura, Determination of total sulfur at microgram per gram levels in geological materials by oxidation of sulfur into sulfate with in situ generation of bromine using isotope dilution high resolution ICPMS, *Anal. Chem.*, **73**, 2547–2553, 2001.

Makishima, A., M., Nakanishi & E., Nakamura, A group separation method of ruthenium, palladium, rhenium, osmium iridium and platinum using their bromo complexs and an anion exchange resin, *Anal. Chem.*, **73**, 5240–5246, 2001.

Makishima, A., K., Kobayashi & E., Nakamura, Determination of Cr, Ni, Cu and Zn in milligram samples of geological materials using isotope dilution high resolution ICP-MS, *Geostand., Newslett.*, **26**, 41–51, 2002

Moriguti, T., & E. Nakamura, High-yield Li separation and the precise isotopic analysis for natural rock and aqueous samples, *Chem. Geol.*, **145**, 91–104, 1998a.

Moriguti, T., & E. Nakamura, Across-arc variation of Li isotopes in arc lavas and implications for crust/mantle recycling at subduction zones, *Earth Planet. Sci. Lett.*, **163**, 167–174, 1998b.

Nakamura, E., T. Ishikawa, J.-L. Birck, & C.J. Allègre, Precise B isotopic analysis of natural rock samples using a B-mannitol complex, *Chem. Geol.*, **94**, 193–204, 1992.

Nakamura, E & I. Kushiro, Trace element diffusion in jadite and diopside melts at high pressures and its geochemical implication, *Geochim, Cosmochim. Acta*, **62**, 3151–3160, 1998.

Nakano, T., & E. Nakamura, Static multicollection of $Cs_2BO_2^+$ ions for precise B isotope analysis with positive thermal ionization mass spectrometry. *Int. J. Mass Spectrom. Ion Processes*, **176**, 13–22, 1998.

Nakano, T., & E. Nakamura, B isotope geochemistry of metasedimentary rocks and tourmalines in a subduction-zone metamorphic suite. *Phys. Earth Planet. Interior*, **127**, 233–252, 2001.

Papanastassiou, D.A. & G. J. Wasserburg, Initial strontium isotopic abundances and the resolution of small time differences in the formation of planetary objects, *Earth Planet. Sci. Letters*, **8**, 1-9, 1969.

Potts, P.J. A handbook of silicate rock analysis, *Blackie & Son*, pp. 622, 1987.

Shen, J.J., D. A. Papanastassiou & G. J. Wasserburg, Precise Re-Os determinations and systematics of iron meteorites, *Geochim. Cosmochim. Acta*, **60**, 2887–2900, 1996.

Shimizu, N. & S. R. Hart, Applications of the ion microprobe to geochemistry and cosmochemistry, *Annu. Rev. Earth Planet. Sci.*, **10**, 483–526, 1982.

Todt, W., Cliff, R. A., Hanser, A., & Hofmann, A. W., Evaluation of a ^{202}Pb-^{205}Pb double spike for high-precision Pb isotope analysis, *Geophysical Monograph*, **95**, 429–437, 1996.

Tuttas, D., & Habfast, K., High precision Pb isotope ratio measurements, *Finnigan MAT Appl. Rep.*, **51**, 3–19, 1982.

Woodhead, J. D., Volker, F., & McCulloch, M. T., Routine Pb isotope determinations using a Pb-207-Pb-204 double spike: a long-term assessment of analytical precision and accuracy, *Analyst*, **120**,

35–39, 1995.

Yokoyama, T., A. Makishima & E. Nakamura, Evaluation of the coprecipitation of incompatible trace elements with fluoride during silicate rock dissolution by acid digestion, *Chem. Geol.*, **157**, 175–187, 1999.

Yokoyama, T., A. Makishima & E. Nakamura, Precise analysis of $^{234}U/^{238}U$ ratio using UO_2^+ ion with thermal ionization mass spectrometry for natural samples, *Chem. Geol.*, **181**, 1–12, 2001.

Yoshikawa, M. & E. Nakamura, Precise isotope determination of trace amounts of Sr in magnesium-rich samples, *Japan. J. Min. Pet. Econ. Geol.* **88**, 548–561, 1993.